

**BROADSIDE-COUPLED
PATCH DIRECTIONAL COUPLER**

TEW LEE NI

**A project report submitted in partial fulfilment of the
requirements for the award of the degree of
Bachelor (Hons) of Electronic and Communications Engineering**

**Faculty of Engineering and Science
Universiti Tunku Abdul Rahman**

SEPTEMBER 2012

DECLARATION

I hereby declare that this project report is based on my original work except for citations and quotations which have been duly acknowledged. I also declare that it has not been previously and concurrently submitted for any other degree or award at UTAR or other institutions.

Signature : _____

Name : TEW LEE NI

ID No. : 09UEB07810

Date : _____

APPROVAL FOR SUBMISSION

I certify that this project report entitled “**BROADSIDE-COUPLED PATCH DIRECTIONAL COUPLER**” was prepared by **TEW LEE NI** has met the required standard for submission in partial fulfilment of the requirements for the award of Bachelor of Engineering (Hons.) Electronic and Communications Engineering at University Tunku Abdul Rahman.

Approved by,

Signature : _____

Supervisor: Dr. Lim Eng Hock

Date : _____

The copyright of this report belongs to the author under the terms of the copyright Act 1987 as qualified by Intellectual Property Policy of University Tunku Abdul Rahman. Due acknowledgement shall always be made of the use of any material contained in, or derived from, this report.

© 2012, Tew Lee Ni. All right reserved.

ACKNOWLEDGEMENTS

I would like to thank everyone who had contributed to the successful completion of this project. I would like to express my gratitude to my research supervisor, Dr. Lim Eng Hock for his invaluable advice, guidance and his enormous patience throughout the development of the research.

In addition, I would also like to express my gratitude to my loving parent and friends who had helped and given me encouragement and auspice in my FYP process. I also want to thank my senior give me some opinion when I doing the simulation. They also provide some important information during the process.

BROADSIDE-COUPLED PATCH DIRECTIONAL COUPLER

ABSTRACT

Directional couplers are passive reciprocal networks. It is a four-port network where all four ports are ideally matched and lossless. The wave incident in port 1 couples power into ports 2 and 3 but not into port 4. Nowadays, these components are essential to all communication systems as they play an important role in the monitoring and measurement of signal samples within an assigned operating frequency. In the first part of the project is to propose a broadside-coupled patch directional coupler. The substrate used is RO4003C with the $\epsilon_r = 3.38$ and $H = 0.8128$ mm or 32 mil. A travelling-wave sectorial slot resonator with three ports is presented in the second part. High Frequency Structure Simulator (HFSS) has been used to optimize the magnitude of the directional coupler. After that, the proposed directional coupler are fabricated and measured by using Vector Network Analyzer (VNA) in the laboratory. The experimental results have agreed well with simulation results. Parameter analysis has been conducted on the proposed directional coupler in order to study the effects of different design parameters. Discussion and recommendation have been made after each parameter analysis.

TABLE OF CONTENTS

DECLARATION	ii
APPROVAL FOR SUBMISSION	iii
ACKNOWLEDGEMENTS	v
ABSTRACT	vi
TABLE OF CONTENTS	vii
LIST OF TABLES	ix
LIST OF FIGURES	x
LIST OF SYMBOLS / ABBREVIATIONS	xiv

CHAPTER

1	INTRODUCTION	1
	1.1 Background	1
	1.2 Aims and Objectives	5
	1.3 Project Motivation	6
2	LITERATURE REVIEW	7
	2.1 Background	7
	2.2 Directional Coupler	7
	2.2.1 Conventional Coupled-line Directional Coupler	10
	2.2.2 Hybrid Coupler	12
	2.3 Dual-band Filter with Stepped-impedance Resonators	17
	2.4 Wideband Rectangular-shaped Directional coupler	21
	2.5 Dual-mode Bandpass Filter Using Slot Resonator	26
	2.6 Introduction of Simulation Tools	29

2.6.1	High Frequency Structure Simulator	29
2.6.2	Microwave Office	30
3	BROADSIDE-COUPLED PATCH DIRECTIONAL COUPLER	31
3.1	Background	31
3.2	Simulation Stage	31
3.3	Fabrication Stage	32
3.4	Experiment Stage	33
3.5	Broadside-coupled Patch Directional Coupler	33
3.5.1	Configuration	34
3.5.2	Result and Discussion	36
3.5.3	Parametric Analysis	39
4	TRAVELLING-WAVE SECTORIAL SLOT RESONATOR	56
4.1	Background	56
4.1.1	Series RLC Resonator	57
4.1.2	Parallel RLC Resonator	58
4.2	Configuration	60
4.3	Results and Discussion	62
4.4	Parametric Analysis	63
5	CONCLUSION AND RECOMMENDATIONS	79
5.1	Achievement	79
5.2	Future Work	79
5.3	Conclusion	80
	REFERENCES	81

LIST OF TABLES

TABLE	TITLE	PAGE
1.1	Frequency band designation.	2
1.2	Microwave Frequency band designation.	3
3.1	Comparison of the experiment and simulation results	39

LIST OF FIGURES

FIGURE	TITLE	PAGE
1.1	Microstrip structure	3
2.1	Ideal Directional Coupler	8
2.2	Conventional coupled-line directional coupler structure	10
2.3	Even- and odd-mode characteristic impedance of coupled-line directional coupler	12
2.4	Branch-line coupler	13
2.5	Even mode excitation	14
2.6	Odd mode excitation	15
2.7	Branch-line circuit in normalized form	15
2.8	Configuration	18
2.9	S-parameter simulation obtained by Sonnet	19
2.10	S-parameter simulation obtained by HFSS	19
2.11:	Current density distribution of two-band centre frequency	20
2.12	Current density distribution of three transmission zeros of filter	20
2.13	Overall view of coupler configuration	21
2.14	Top view of coupler structure	22
2.15	The designed coupler dimension.	23

2.16	Length analysis for return loss	24
2.17	Length analysis for through characteristic	24
2.18	Length analysis for coupling characteristic	25
2.19	Simulated S-parameter performance	25
2.20	Proposed dual-mode filter configuration. (a) Total view, (b) Slot-	27
2.21	Prototype of the dual-mode SSLR filter	28
2.22	S-parameter of the simulation and experiment	28
3.1	Dimension of multiple output faces coupler directional coupler	35
3.2	Prototype of the proposed multi-port directional coupler.	36
3.3	Magnitude response of multiple output faces coupler directional coupler	37
3.4	Effect of width W_1 on the proposed directional coupler	40
3.5	Effect of width W_2 on the proposed directional coupler	41
3.6	Effect of length L_1 on the proposed directional coupler	42
3.7	Effect of length L_2 on the proposed directional coupler	43
3.8	Effect of length L_3 on the proposed directional coupler	44
3.9	Effect of length L_4 on the proposed directional coupler	45
3.10	Effect of gap G_1 on the proposed directional coupler	46
3.11	Effect of gap G_2 on the proposed directional coupler	47

3.12	Effect of substrate S_1 on the proposed directional coupler	48
3.13	Effect of substrate S_2 on the proposed directional coupler	49
3.14	Effect of substrate size S_1 and S_2 on the proposed directional coupler	50
3.15	Effect of substrate thickness H_1 on the proposed directional coupler	51
3.16	Effect of length L_2 and L_3 on the proposed directional coupler	52
3.17	Effect of length L_1 and L_4 on the proposed directional coupler	53
3.18	Effect of width W_1 and W_2 on the proposed directional coupler	54
3.19	Effect of gap G_1 and G_2 on the proposed directional coupler	55
4.1	Series RLC resonator circuit	57
4.2	Input impedance magnitude of a series RLC resonator	58
4.3	Parallel RLC resonant circuit	59
4.4	The input impedance magnitude of the parallel RLC resonator.	60
4.5	Configuration of the proposed resonator (a) Top-down view (b) Bottom-layer structure (c) top-layer structure (d) middle-layer structure	62
4.6	S-parameter of the proposed resonator	63
4.7	Effect of radius R_1 on the proposed resonator	64
4.8	Effect of radius R_2 on the proposed resonator	65
4.9	Effect of radius R_3 on the proposed resonator	66
4.10	Effect of width W_1 on the proposed resonator	67
4.11	Effect of width W_2 on the proposed resonator	68

4.12	Effect of width W_3 on the proposed resonator	69
4.13	Effect of size S_1 on the proposed resonator	70
4.14	Effect of size S_2 on the proposed resonator	71
4.15	Effect of size S_1 and S_2 on the proposed resonator	72
4.16	Effect of radius R_1 and R_2 on the proposed resonator	73
4.17	Effect of width W_1 , W_2 and W_3 on the proposed resonator	74
4.18	Effect of thickness H_1 on the proposed resonator	75
4.19	Effect of gap G_1 on the proposed resonator	76
4.20	Effect of gap G_2 on the proposed resonator	77
4.21	Effect of gap G_1 and G_2 on the proposed resonator	78

LIST OF SYMBOLS / ABBREVIATIONS

λ	Wavelength, m
f	Frequency, Hz
c	Speed of light, m/s
ϵ_r	Dielectric constant
ϵ_{eff}	Effective dielectric constant
H	Thickness of substrate, mm
W	Width of microstrip lines, mm
L	Length of microstrip lines, mm
Z_o	Characteristic impedance, Ω
Z_{in}	Input impedance, Ω
S_{11}	Reflection coefficient, dB
S_{21}	Insertion loss, dB
S_{31}	Insertion loss, dB
S_{41}	Isolation, dB

CHAPTER 1

INTRODUCTION

1.1 Background

In microwaves engineering, the term “microwave” mean the range of radio frequencies between 300MHz and 30GHz. The applications of microwave most concern in radar, communication and wireless systems. With Alexander Popov and Sir Oliver Lodge laying the groundwork for Guglielmo Marconi’s wireless radio developments in the early 20th century, Radio Frequency (RF) and wireless have been around for over a century.

Microwaves are highly developed in radar and communications system. For example, radar systems are used to detect and locate air, ground or seagoing targets and for air-traffic control systems, missile tracking radars, automobile collision-avoidance systems, weather prediction, motion detectors and a wide variety of remote sensing systems. Microwave communication systems handle a large fraction of the world’s international and other long-haul telephone, data and television transmissions.

Nowadays many developed wireless telecommunications systems operating frequencies are between ranges 1.5 to 9.4 GHz, such as direct broadcast satellite (DBS) television, personal communications systems (PCSs), wireless local area computer networks (WLANS), cellular video (CV) systems and global positioning satellite (GPS) systems.

Table 1.1 and 1.2 below are showing the frequency band designation and microwave frequency band designation. Table 1.1 shows the relationship between frequency and wavelength. Frequency (f) and wavelength (λ) are inversely proportional to each other and both related with speed of light (C) through a medium can prove by below equation:

$$C = f \times \lambda$$

Table 1.1: Frequency band designation.

Frequency, f	Wavelength, λ	Band
30 – 300 Hz	$10^4 - 10^3$ km	Extremely low frequency (ELF)
300 – 3000 Hz	$10^3 - 10^2$ km	Voice frequency (VF)
3 – 30 kHz	100 – 10 km	Very low frequency (VLF)
30 – 300 kHz	10 – 1 km	Low frequency (LF)
0.3 – 3 MHz	1 – 0.1 km	Medium frequency (MF)
3 – 30 MHz	100 – 10 m	High frequency (HF)
30 – 300 MHz	10 – 1 m	Very high frequency (VHF)
300 – 3000 MHz	100 – 10 cm	Ultra-high frequency (UHF)
3 – 30 GHz	10 – 1 cm	Super-high frequency (SHF)
30 – 300 GHz	10 – 1 mm	Extremely high frequency (EHF)

Obtained from: <http://www.ni.com/white-paper/3541/en>

Table 1.2: Microwave Frequency band designation.

Frequency, f (GHz)	Letter Band Designation
1 – 2	L band
2 – 4	S band
4 – 8	C band
8 – 12.4	X band
12.4 – 18	Ku band
18 – 26.5	K band
26.5 – 40	Ka band

Obtained from: <http://www.ni.com/white-paper/3541/en>

To convey the microwave frequency signal, a microstrip technology will be used. Microstrip is a planar transmission line which similar to stripline and coplanar waveguide. Microwave components can be found in antennas, directional couplers, filters and power dividers which formed from microstrip. Microstrip was developed by ITT Ferearl Telecommunications Laboratories in Nutley New Jersey, as a competitor to stripline (first published by Grieg and Engelmann in the December 1952 IRE proceedings).

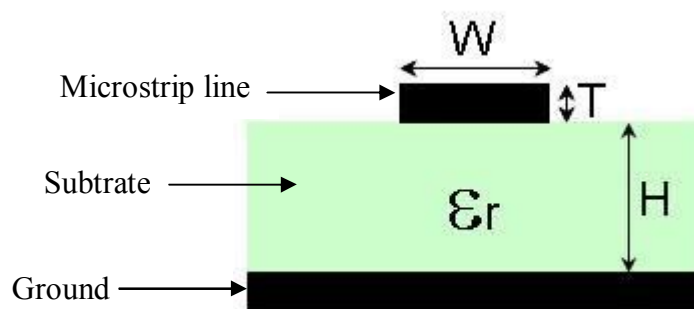
**Figure 1.1: Microstrip structure**

Figure 1.1 shows the general microstrip structure. Microstrip consist of conductive microstrip line and a ground plane which separated by a dielectric layer called

substrate. To design a microstrip, width (W) and thickness (T) of conductive microstrip line and height (H) of the substrate are very important. ϵ_r represent the dielectric constant or relative permittivity of the substrate. In this project we will use microstrip technology because all active components can be mounting on the top of the board. Apart from microstrip are much less expensive, lighter and more compact.

In theoretical, effective dielectric constant (ϵ_{eff}) and characteristics impedance (Z_0) of the microstrip line will be introduced. To find effective dielectric constant, below equation can be use.

$$\epsilon_{eff} = \frac{\epsilon_r + 1}{2} + \frac{\epsilon_r - 1}{2} \frac{1}{\sqrt{1 + 12H/W}}$$

By using dimension of microstrip line H/W, characteristic impedance can calculated as

$$Z_0 = \begin{cases} \frac{60}{\sqrt{\epsilon_{eff}}} \ln \left(\frac{8H}{W} + \frac{W}{H} \right) & \text{when } \left(\frac{W}{H} \right) \leq 1 \\ \frac{120\pi}{\sqrt{\epsilon_{eff}} \times \left[\frac{W}{H} + 1.393 + \frac{2}{3} \ln \left(\frac{W}{H} + 1.444 \right) \right]} & \text{when } \left(\frac{W}{H} \right) \geq 1 \end{cases}$$

By given the characteristic impedance and dielectric constant, dimension can be calculated by below equation

$$\frac{W}{H} = \begin{cases} \frac{8e^A}{e^{2A} - 2} \\ \frac{2}{\pi} \left[B - 1 - \ln(2B - 1) + \frac{\epsilon_r - 1}{2\epsilon_r} \left\{ \ln(B - 1) + 0.39 - \frac{0.61}{\epsilon_r} \right\} \right] \end{cases}$$

Where

$$A = \frac{Z_0}{60} \sqrt{\frac{\epsilon_r + 1}{2} + \frac{\epsilon_r - 1}{\epsilon_r + 1} \left(0.23 + \frac{0.11}{\epsilon_r}\right)}$$

$$B = \frac{377\pi}{2Z_0\sqrt{\epsilon_r}}$$

1.2 Aims and Objectives

Main objective of this project is to design a new microstrip directional coupler technique which is patch-coupled directional coupler to achieve a wider bandwidth. Author needs to understand fundamental theory of microstrip directional coupler before start to implement the project. Author can get the related journals or articles through IEEE Xplore database under the University Tunku Abdul Rahman (UTAR) OPAC system. Besides that, author also can get information or knowledge from the websites or Pozar book which provided in the library of UTAR.

The first proposed idea is to design a broadside-coupled patch directional coupler. The designed directional coupler resonates between 2 to 7 GHz. This design is one of the latest techniques of the microwave component. Coupler is a dual-mode directional coupler which has wider bandwidth. Obviously, the more modes a directional coupler has, the wider bandwidth is.

Throughout this project, author has gained better understanding and knowledge of passive microwave components such as directional couplers, filters and power dividers. Apart from that, author learned how to use the HFSS software to design directional coupler. Authors can also using freelance software to compare the result of simulation and experimental results. In the experiment, when students facing any problem, students must try to solve the problem so that can get nearest or better result compare to simulation result.

1.3 Project Motivation

Motivation of this project is to design a new microstrip directional coupler. After this project, students understand the background and function of directional coupler. So in the future, student can design more microwave components depending on the needed of industry. In this experiment, students are going to design a microstrip directional coupler that has wider bandwidth and higher performance.

CHAPTER 2

LITERATURE REVIEW

2.1 Background

Firstly, directional coupler will be introduced in this chapter. After that, a new design methodology will also introduce which was published in IEEE Xplore database. The design will be simulate and discuss by author. Lastly, simulation tools that have been used in this project will be introduced such as High Frequency Structure Simulator (HFSS), Microwave Office and Freelance Graphics software.

2.2 Directional Coupler

Directional couplers are passive reciprocal networks. It is a four-port network where all four ports are ideally matched and lossless. Directional couplers can be realized in microstrip, stripline, coax and waveguide. Directional couplers are used to sample a signal, incident and reflected waves. Generally, couplers use distributed properties of microwave circuits which coupling feature is a quarter or multiple quarter-wavelengths. Purposes of directional couplers are used in RF (radio frequency) and microwave routing for isolation, separating and combining signals.

Applications of directional coupler are providing a signal sample for measurement or monitor, feedback, combining feeds to and from antenna. Directional coupler also providing taps for cable distributed system such as cable television, separating

transmitted and received signals on telephone lines. Figure 2.1 shows an ideal directional coupler schematic where port 1 is the input port, port 2 is through port, port 3 is coupled port and port 4 is isolation port. The wave incident in port 1 couples power into ports 2 and 3 but not into port 4.

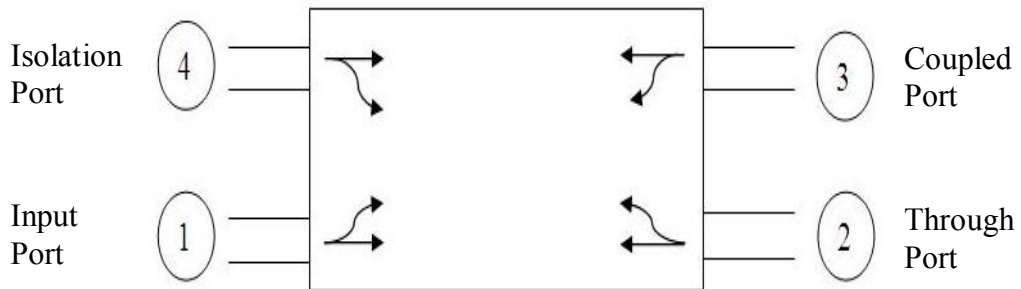


Figure 2.1: Ideal Directional Coupler

Directional coupler has three specifications which is coupling (C), directivity (D) and isolation (I). Coupling is ratio of input power to coupler power. Directivity is ratio of coupled power to the power at isolated port. Isolation is ratio of input power to power flow out of the isolated port. Isolation is also known as the sum of coupling factor and directivity of directional coupler.

$$C = 10 \log \frac{P_1}{P_3} \quad (\text{dB})$$

$$D = 10 \log \frac{P_3}{P_4} \quad (\text{dB})$$

$$I = 10 \log \frac{P_1}{P_4} = 10 \log \frac{P_1}{P_3} \frac{P_3}{P_4} = 10 \log \frac{P_1}{P_3} + 10 \log \frac{P_3}{P_4} \quad (\text{dB})$$

$$I = C + D \quad (\text{dB})$$

For a four-port network, S-matrix of a reciprocal and matched network has the following form:

$$\bar{S} = \begin{bmatrix} 0 & S_{12} & S_{13} & S_{14} \\ S_{21} & 0 & S_{23} & S_{24} \\ S_{31} & S_{32} & 0 & S_{34} \\ S_{41} & S_{42} & S_{43} & 0 \end{bmatrix}$$

If the network is matched at every port, then $S_{11} = S_{22} = S_{33} = S_{44} = 0$. It mean $\Gamma_1, \Gamma_2, \Gamma_3$ and $\Gamma_4 = 0$ when all other ports are terminated in Z_0 . If networks are reciprocal, then $S_{21} = S_{12}, S_{31} = S_{13}, S_{32} = S_{23}, S_{41} = S_{14}, S_{42} = S_{24}, S_{43} = S_{34}$. A symmetry coupler phases have amplitude β which is chosen equal. So, S-matrix for this network is

$$\bar{S} = \begin{bmatrix} 0 & \alpha & j\beta & 0 \\ \alpha & 0 & 0 & j\beta \\ j\beta & 0 & 0 & \alpha \\ 0 & j\beta & \alpha & 0 \end{bmatrix}$$

An asymmetry coupler phases will also have amplitude β but chosen in 180° apart. S-matrix is:

$$\bar{S} = \begin{bmatrix} 0 & \alpha & \beta & 0 \\ \alpha & 0 & 0 & \beta \\ \beta & 0 & 0 & \alpha \\ 0 & \beta & \alpha & 0 \end{bmatrix}$$

When a network is in reciprocal, lossless and matched four-port network, the network will consider as a directional coupler.

In directional coupler, there are two types of losses must concern which is insertion loss and coupling loss. Insertion loss is signal pass through from port 1 to port 2 and relate with environment that joins the two ports. While, coupling loss occur when signal pass through from port 1 to port 3 and it is relate to the quantity of power coupled.

2.2.1 Conventional Coupled-line Directional Coupler

Conventional coupled-line directional coupler is one of the common methods to design directional coupler. Figure 2.2 shows the conventional coupled-line directional coupler structure.

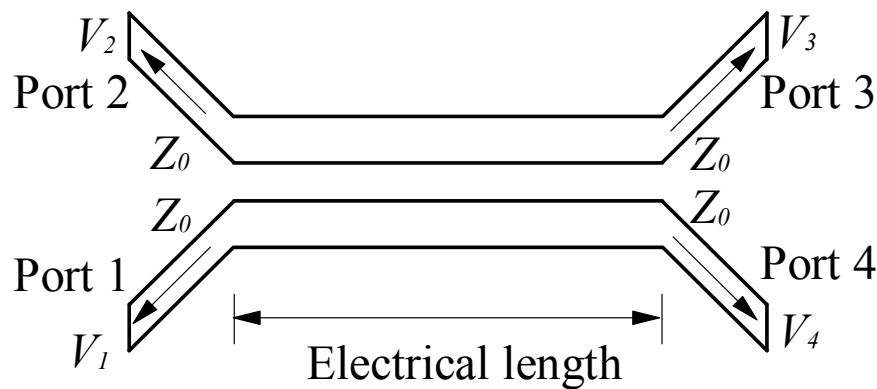


Figure 2.2: Conventional coupled-line directional coupler structure

In this structure, coupling level between the ports is due to interaction of electromagnetic fields along transmission lines which have been placed in close proximity. In addition, it can be named as TEM-mode quarter-wavelength directional coupler. (Leo Young, M.A., Dr. Eng., 1963).

One method to analyze multi-port transmission line circuits such as coupled line is through even and odd mode analysis. In this case, circuit input voltage is split into two, even (symmetric) and odd (anti-symmetric) mode. Z_{0e} is the characteristic impedance of a transmission line under even mode operation and Z_{0o} is characteristic impedance lines under the odd mode excitation.

Midband amplitude coupling factor, c is given in terms of even mode characteristic impedance, Z_{0e} and odd mode characteristic impedance, Z_{0o} such as:

$$c = \frac{Z_{0e} - Z_{0o}}{Z_{0e} + Z_{0o}}$$

Characteristic impedance Z_0 is express in terms as:

$$Z_0 = \sqrt{Z_{0e}Z_{0o}}$$

According to all the equations above, even and odd mode impedances can be written as :

$$Z_{0e} = Z_0 \sqrt{\frac{1+c}{1-c}}$$

and

$$Z_{0o} = Z_0 \sqrt{\frac{1-c}{1+c}}$$

With above equation, we can determine the width and separation of lines for given coupling coefficient. Figure 2.3 shows even- and odd-mode characteristic impedance that has been tabulated by Pozar, with a complete solution for the microstrip lines. But only for $\epsilon_r = 10$. (David M. Pozar, 1998). Parameters used in the graph are represented as below:

S = Separation

W = Width of Microstrip lines

D = Dielectric thickness

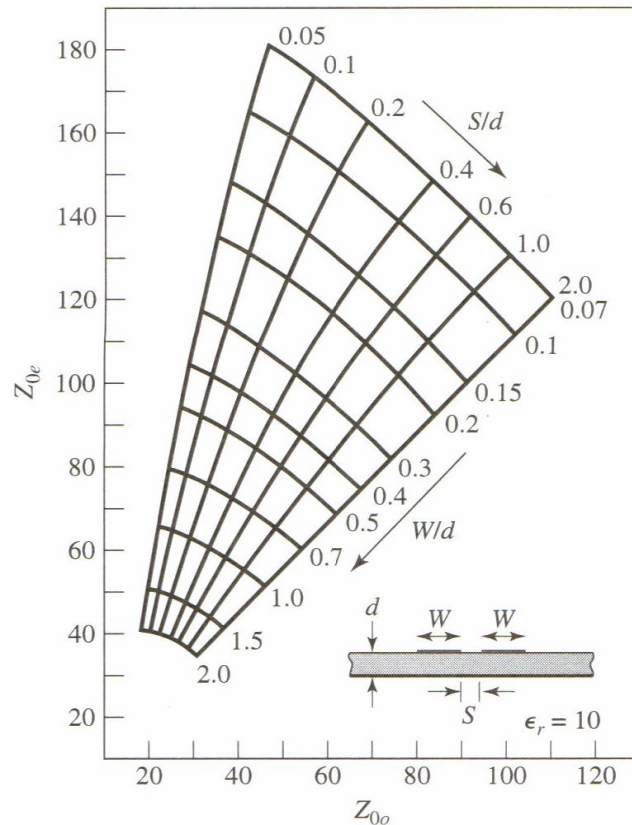


Figure 2.3: Even- and odd-mode characteristic impedance of coupled-line directional coupler

2.2.2 Hybrid Coupler

Directional coupler can be made in many different forms such as waveguide coupler, hybrid coupler, coupled transmission line form and etc. Hybrid coupler is a special form in directional coupler which has coupling factor at 3dB and the phase between ports can be either 90° or 180° which called quadratic hybrid and magic-T (rat-race) hybrid.

Quadrature hybrid is a 3dB directional coupler with 90° phase difference in outputs of the through and coupled arms. (David M. Pozar, 2005). Figure 2.4 shows quadrature hybrid structure and also called branch-line coupler. Because all ports are

matches, power pass through port 1 is evenly divided into 90° phase shift between port 2 and port 3 and there is no power entering into port 4.

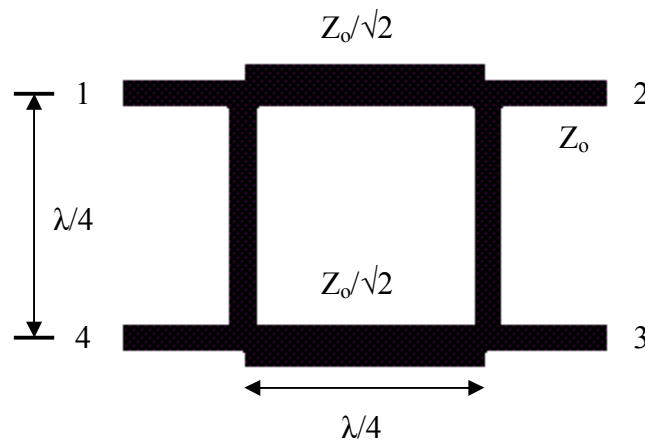


Figure 2.4: Branch-line coupler

Thus, S-matrix can be form as following:

$$S = \frac{-1}{\sqrt{2}} \begin{bmatrix} 0 & j & 1 & 0 \\ j & 0 & 0 & 1 \\ 1 & 0 & 0 & j \\ 0 & 1 & j & 0 \end{bmatrix}$$

Network can be separate into even- and odd mode analysis due to symmetry and antisymmetry of excitation. Figure 2.5 shows even mode excitation and Figure 2.6 shows odd mode excitation. By adding up even and odd mode excitation, it will results the origin excitation as Figure 2.7.

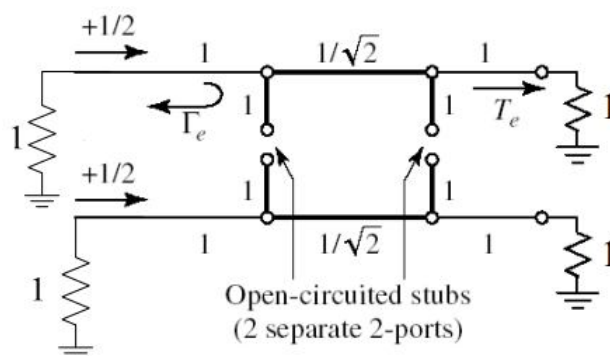
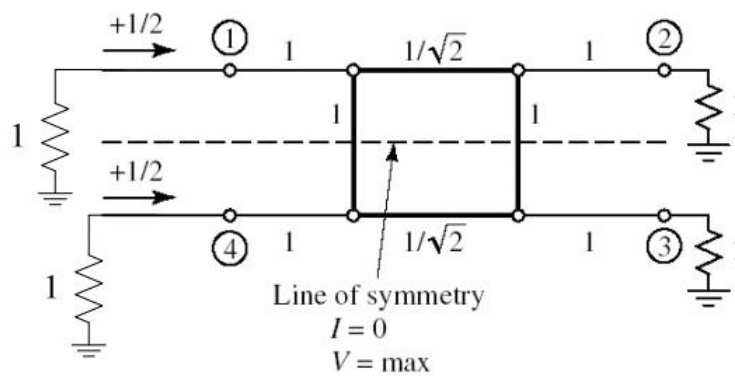
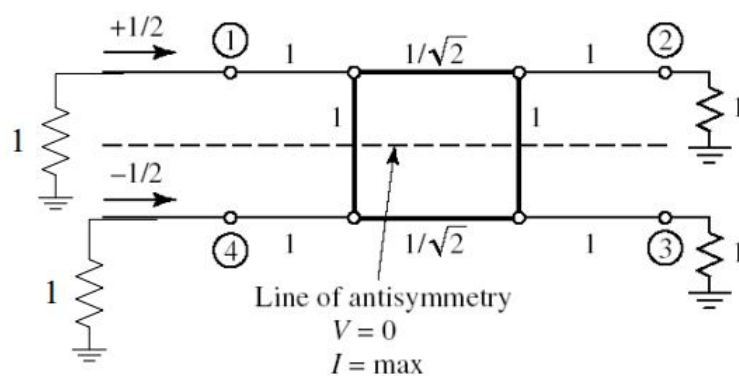


Figure 2.5: Even mode excitation



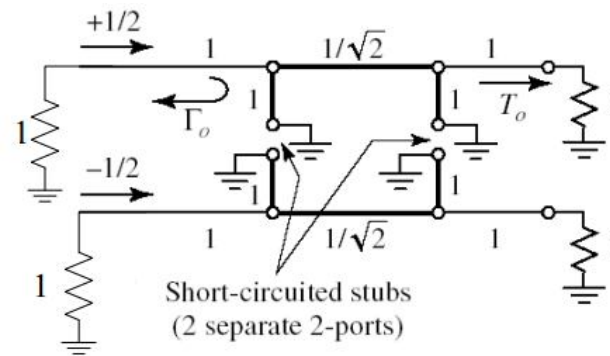


Figure 2.6: Odd mode excitation

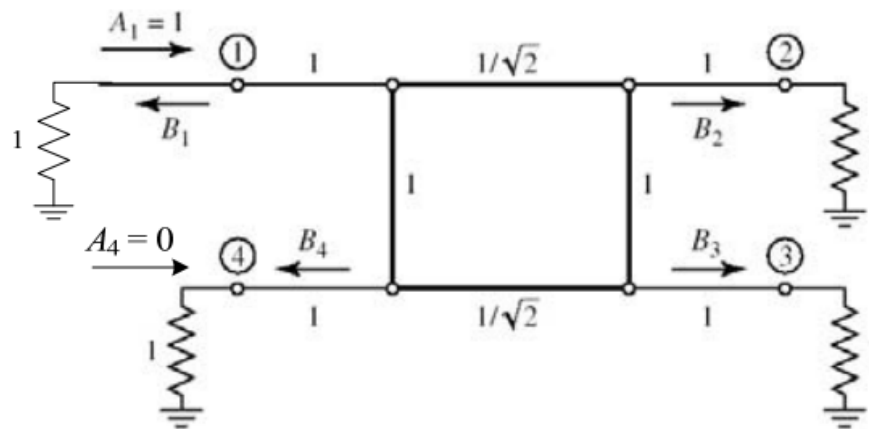


Figure 2.7: Branch-line circuit in normalized form

For even mode analysis, because voltages and currents are in the same above and below the line of symmetry (LOS), so current will be equal zero at LOS. It is an open circuit loads at the ends of the stub. While for odd mode analysis, voltages and currents are opposite values above and below the LOS, it result the voltage equal to zero along LOS which is short circuit loads at the ends of stub.

Since these two ports amplitude of incidents wave is $\pm 1/2$, then the amplitude of emerging wave for each port can be sum up and expressed as following:

$$B_1 = \frac{1}{2}\Gamma_s + \frac{1}{2}\Gamma_o$$

$$B_2 = \frac{1}{2}T_e + \frac{1}{2}T_o$$

$$B_3 = \frac{1}{2}T_e - \frac{1}{2}T_o$$

$$B_4 = \frac{1}{2}\Gamma_e - \frac{1}{2}\Gamma_o$$

Where $\Gamma_{e,o}$ and $T_{e,o}$ represents even and odd mode reflection and transmission coefficient for two networks. By using ABCD matrices, Γ_e and T_e , even mode of two port circuit can be calculated by following:

$$\begin{bmatrix} A & B \\ C & D \end{bmatrix}_e = \begin{bmatrix} 1 & 0 \\ j & 1 \end{bmatrix} \begin{bmatrix} 0 & j\sqrt{2} \\ j\sqrt{2} & 0 \end{bmatrix} \begin{bmatrix} 1 & 0 \\ j & 1 \end{bmatrix} = \frac{1}{\sqrt{2}} \begin{bmatrix} -1 & j \\ j & -1 \end{bmatrix} = \frac{1}{\sqrt{2}} \begin{bmatrix} -1 & j \\ j & -1 \end{bmatrix}$$

Admittance of the shunt open-circuited stub is $Y = j\tan\beta l$. Thus,

$$\Gamma_e = \frac{A+B-C-D}{A+B+C+D} \approx \frac{(-1+j-j+1)/\sqrt{2}}{(-1+j+j-1)/\sqrt{2}} = 0$$

$$T_e = \frac{2}{A+B+C+D} \approx \frac{2}{(-1+j+j-1)/\sqrt{2}} = \frac{-1}{\sqrt{2}}(1+j)$$

It is similarly to obtain odd mode reflection and transmission coefficient.

$$\begin{bmatrix} A & B \\ C & D \end{bmatrix}_o = \frac{1}{\sqrt{2}} \begin{bmatrix} 1 & j \\ j & 1 \end{bmatrix}$$

Odd mode reflection and transmission obtain as below:

$$\Gamma_o = 0$$

$$T_e = \frac{1}{\sqrt{2}} (1 - j)$$

Then $\Gamma_{e,o}$ and $T_{e,o}$ substitute into amplitude of emerging wave for each port and results:

$$B_1 = 0$$

$$B_2 = -\frac{j}{\sqrt{2}}$$

$$B_3 = -\frac{1}{\sqrt{2}}$$

$$B_4 = 0$$

From the results, when port 1 is excited and all other ports terminated in the matched loads, then port 1 is matched ($B_1 = 0$) and it is -90° phase shift from port 1 to port 2, some more one half of the input power is delivered to port 2. Apart from that, there are a 90° phase shift between port 3 and port 2 and one half of the input power is delivered to port 3. At last, port 4 is no power out ($B_4 = 0$).

2.3 Dual-band Filter with Stepped-impedance Resonators

In this sub-chapter, authors will introduce a design of microstrip that has published in IEEE Electronics Letter by H.-J.Yuan and Y.Fan entitled “Compact microstrip dual-band filter with stepped-impedance resonators”. Dual-band filter has become an important device in communication systems because of the increasing demand for wireless communications and the wireless LAN are widely used.

Figure 2.8 shows geometry and dimensions of the filter. Filter substrate with size of 52.2 mm and 40 mm, thickness of 1 mm, and relative permittivity of 9.2. This filter consists of a stepped-impedance resonator and the quarter-wavelength impedance

matching line. The size of the wavelength depends on the 50Ω characteristic impedance. To reduce the size of the filter with effectively, the input and output need uses a tortuous feeder structure to reduce it. (H.-J.Yuan and Y.Fan, November 2011).

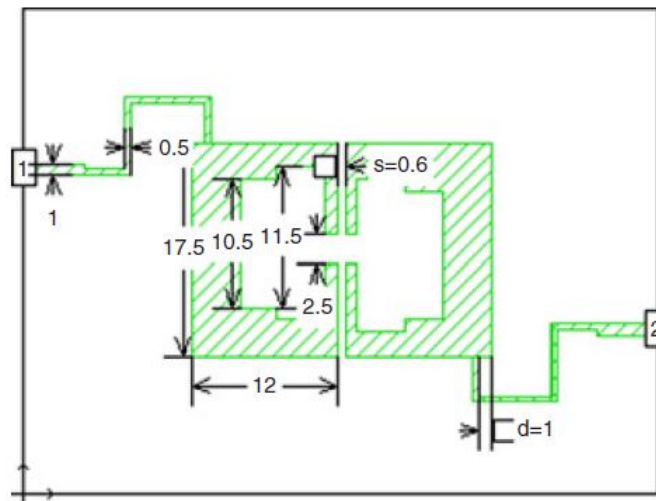


Figure 2.8: Configuration

By using input and output structure in Figure 2.8, author use Sonnet software to simulate S-parameter results as shown in Figure 2.9. From S-parameter, first band's return loss is less than -21.97 dB and second band's return loss is -22.23 dB. Apart from that, there are three transmission zeros at 1.18, 2.36 and 3.32 GHz, respectively. Their attenuation is -75.36 , -62.64 and 49.52 dB, respectively.

While Figure 2.10 shows S-parameter simulation obtained by HFSS. Results are similar but position of the first and second band's return loss locate at different values. Three transmission zeros is quite near to the results simulation by Sonnet. (H.-J.Yuan and Y.Fan, November 2011).

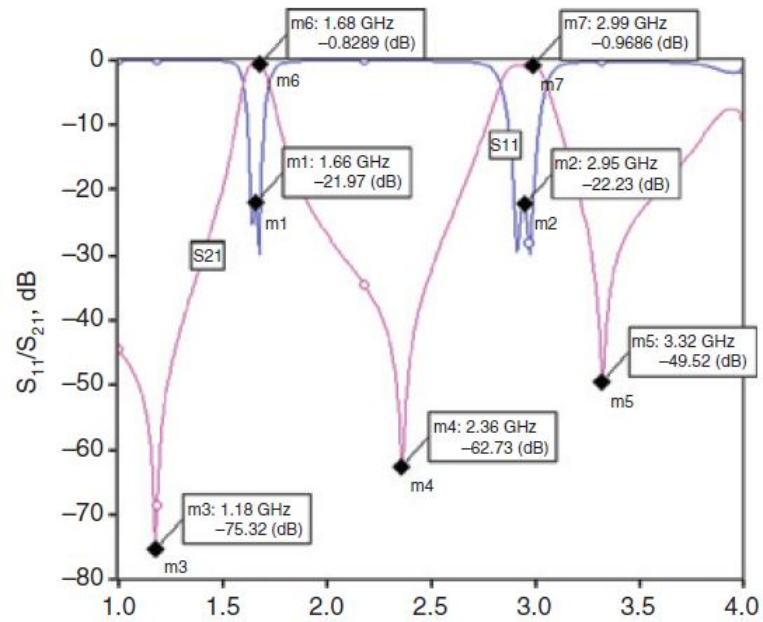


Figure 2.9: S-parameter simulation obtained by Sonnet

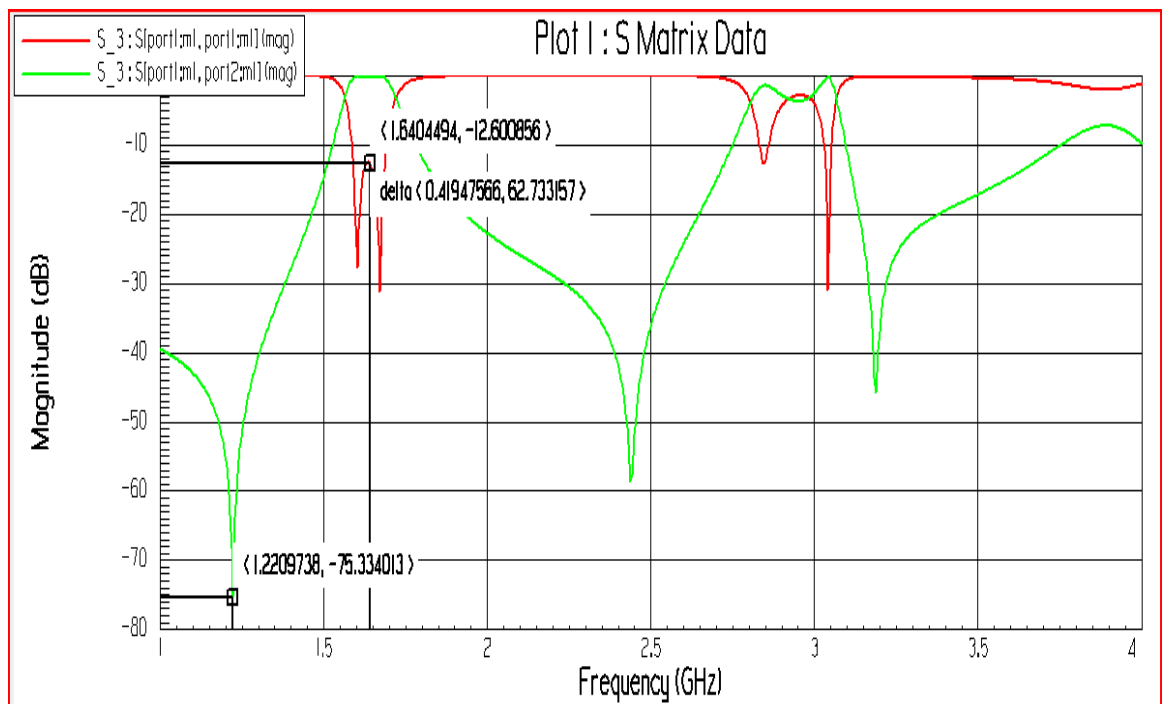


Figure 2.10: S-parameter simulation obtained by HFSS

Figure 2.11 shows current density at first resonant and second resonance frequency which is 1.66 and 2.95 GHz. While Figure 2.12 shows current density distribution of three transmission zeros of the filter.

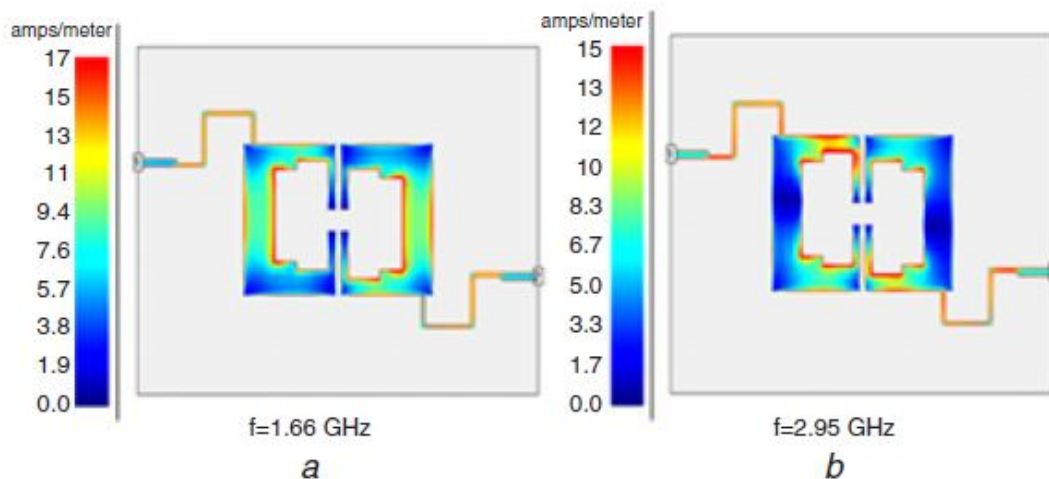


Figure 2.11: Current density distribution of two-band centre frequency

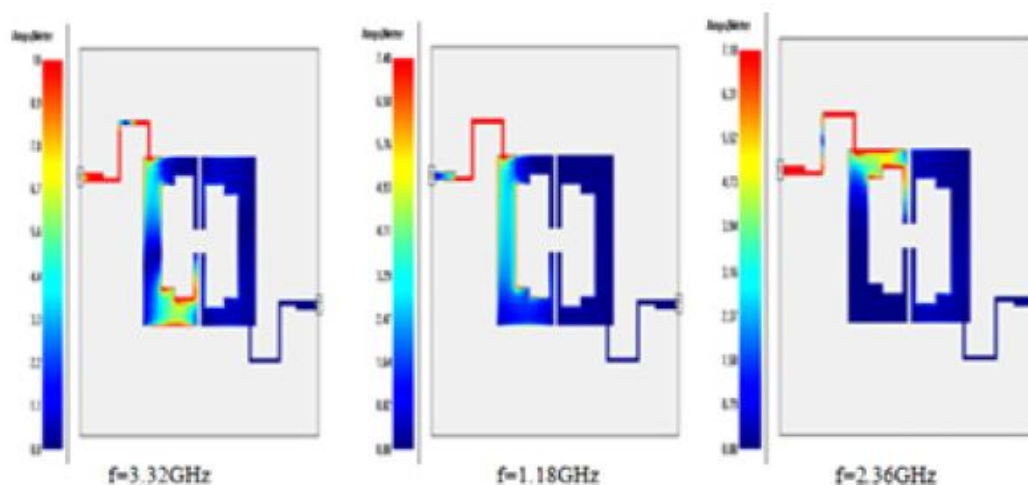


Figure 2.12: Current density distribution of three transmission zeros of filter

At the end, this filter has proposed and analysed by author. Filter has many characteristics such as simple structure and good stop band. Filter can widely use in communication systems.

2.4 Wideband Rectangular-shaped Directional coupler

This design presents of three-section rectangular-shaped directional coupler. Paper can be found on IEEE Xplore database entitle “Design and Cross-Section Analysis of Wideband Rectangular-Shaped Directional Coupler” by authors S.N.A.M. Ghazali, N.Seman, R.C.Yob, M.K.A.Rahim and S.K.A.Rahim. This design offers a tight coupling of 3dB over the designated frequency band of 2 to 6 GHz.

Proposed coupler consists of two substrates and one common ground plane between the two substrates. Design was formed by rectangular-shaped microstrip line at the top and bottom with rectangular slot at the common ground plane. The overall dimension excluding microstrip ports occupy an area of 50 mm x 20 mm. In this design, they are using CST Microwave Studio simulator to optimize the coupler.

The cross-section analysis was performed in order to study the characteristic of electric field during the odd and even-mode excitation of the coupler. Figure 2.13 shows the overall view of the coupler configuration that shows two substrates are sandwiched by the three conductor layers of top and bottom microstrip patch and one layer of conductive coating in the middle which is the ground plane. While figure 2.14 shows the top view of the coupler. (S.N.A.M. Ghazali, N.Seman, R.C.Yob, M.K.A.Rahim and S.K.A.Rahim, December 2011).

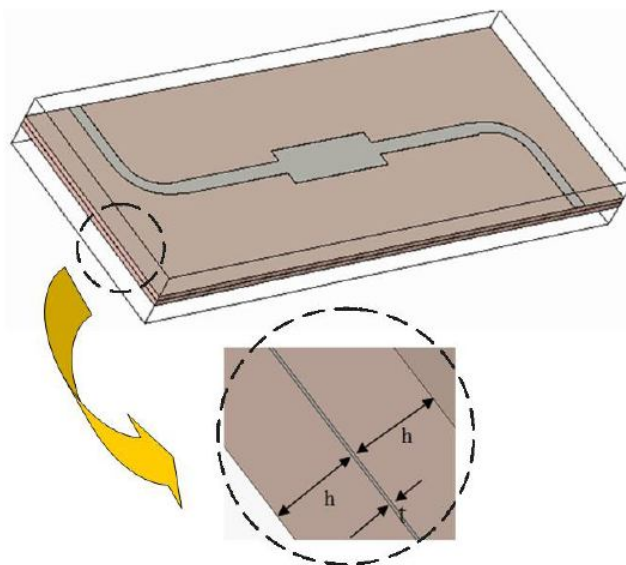


Figure 2.13: Overall view of coupler configuration

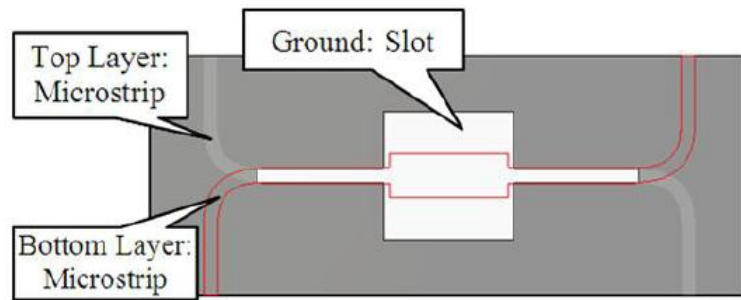


Figure 2.14: Top view of coupler structure

RO4003C substrate with dielectric constant 3.38 and thickness 0.508 mm was used. Dimension of three-section rectangular-shaped coupler as Figure 2.15 and below values.

where

$$wt_1 = wb_1 = 1.35 \text{ mm}$$

$$wt_2 = wb_2 = 3.67 \text{ mm}$$

$$1t_1 = 1t_3 = 1b_1 = 1b_3 = 10.73 \text{ mm}$$

$$1t_2 = 1b_2 = 9.97 \text{ mm}$$

$$wg_1 = 1.18 \text{ mm}$$

$$wg_2 = 10.74 \text{ mm}$$

$$1g_1 = 1g_3 = 10.54 \text{ mm}$$

$$1g_2 = 10.93 \text{ mm}$$

(S.N.A.M. Ghazali, N.Seman, R.C.Yob, M.K.A.Rahim and S.K.A.Rahim, December 2011).

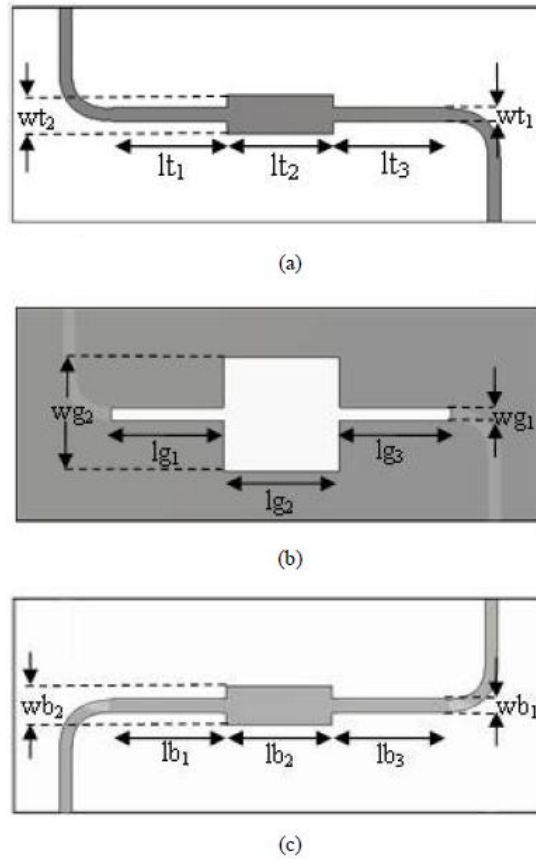


Figure 2.15: The designed coupler dimension.

By vary length of middle section microstrip patch ($1t_2$), it controls frequency range characteristic and the effect of different phase velocities for even and odd propagation modes. While by varied the length of $1t_2$ from 4 mm to 10 mm with step of 2 mm, performance of return loss, through and coupling characteristic are observed as shown in Figure 2.16 to Figure 2.18. (S.N.A.M. Ghazali, N.Seman, R.C.Yob, M.K.A.Rahim and S.K.A.Rahim, December 2011).

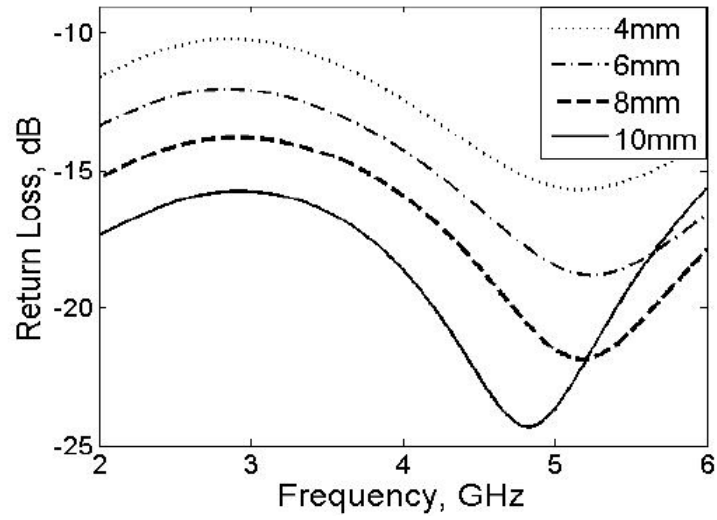


Figure 2.16: Length analysis for return loss

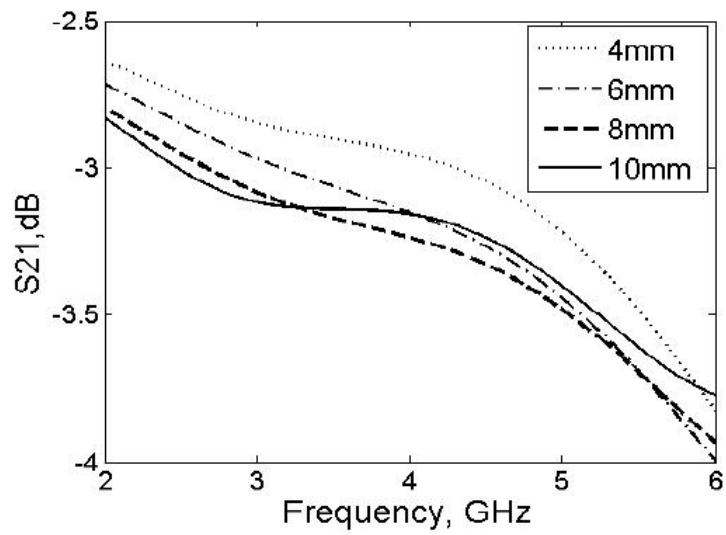


Figure 2.17: Length analysis for through characteristic

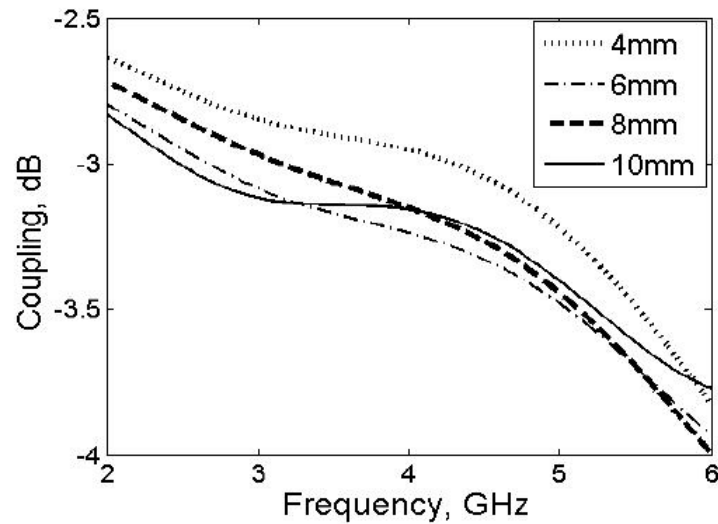


Figure 2.18: length analysis for coupling characteristic

From length analysis, worst performance of return loss was at 4 mm which just slightly better than 10 dB is observed. Meanwhile, through and coupling characteristic does not change much which varied between 3 ± 1 dB. (S.N.A.M. Ghazali, N.Seman, R.C.Yob, M.K.A.Rahim and S.K.A.Rahim, December 2011). Figure 2.18 shows simulation S-parameter performance of rectangular-shaped coupler from 2 to 6 GHz frequency range.

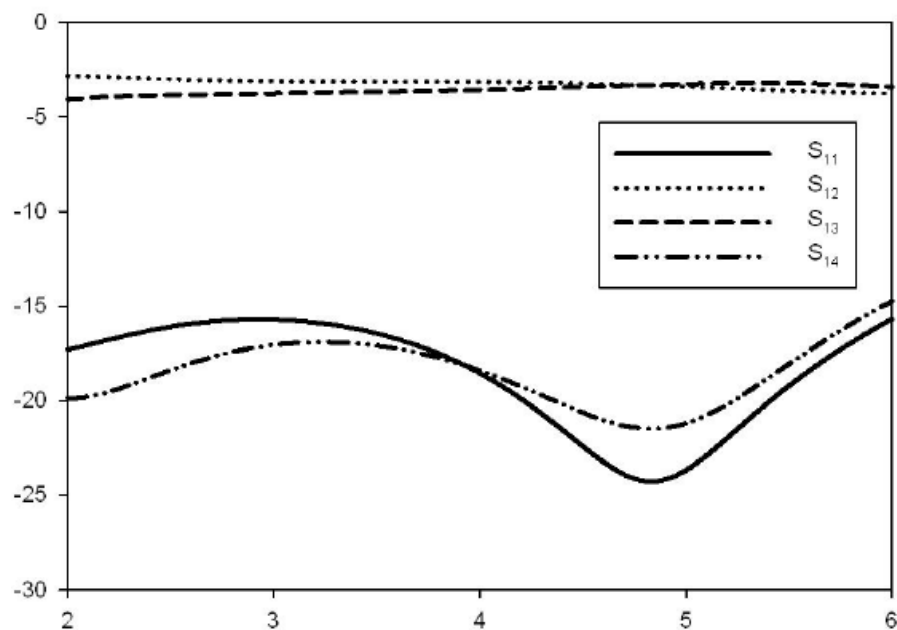


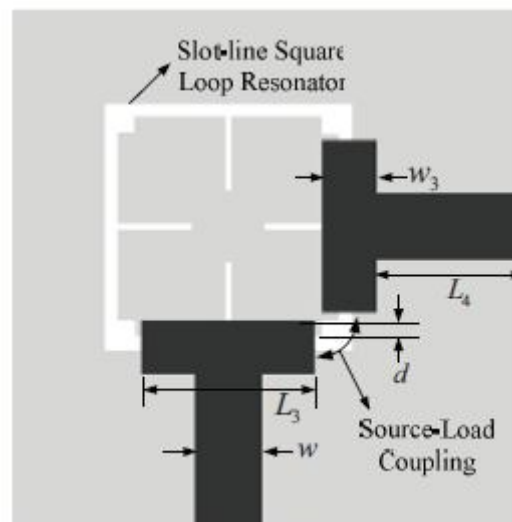
Figure 2.19: Simulated S-parameter performance

This coupler shows simulated return losses at all of its port and isolation between port 1 and 4, and 2 and 3 are better than 15 dB from 2 to 6 GHz. In frequency range, coupling coefficient between ports 1 and 3, and 2 and 4 is $3 \text{ dB} \pm 1$ deviation. At the end, its return loss and isolation have been confirmed for 2 to 6 GHz frequency range.

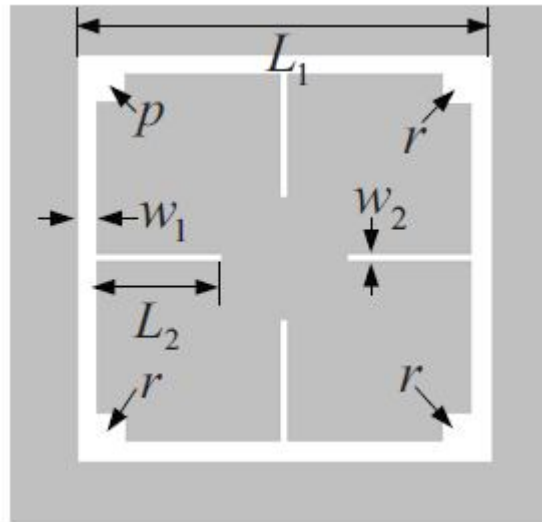
2.5 Dual-mode Bandpass Filter Using Slot Resonator

Microstrip filters with dual-mode property has been widely used in the design of planar microwave filters. Therefore, a dual-mode bandpass filter by using a slot-line square loop resonator is proposed by Bian Wu, Wen Su, Shou-jia Sun and Chang-Hong Liang.

Figure 2.20 shows configuration of the proposed dual-mode filter based on slot-line square loop resonator loaded with patches and stubs, the square loop resonator is defected on the top plane. (Bian Wu, Wen Su, Shou-jia Sun and Chang-Hong Liang, 2012).



(a)



(b)

Figure 2.20: Proposed dual-mode filter configuration. (a) Total view, (b) Slot-line square loop resonator (SSLR) loaded with patches and stubs.

A SSLR dual-mode filter with asymmetrical response is designed and fabricated as shown in figure 2.21, the parameter are chosen as:

$$L_1 = 10 \text{ mm}$$

$$L_2 = 3 \text{ mm}$$

$$L_3 = 7 \text{ mm}$$

$$w_1 = 0.5 \text{ mm}$$

$$w_2 = 0.2 \text{ mm}$$

$$w_3 = 2.2 \text{ mm}$$

$$p = 0.65 \text{ mm}$$

$$r = 0.7 \text{ mm}$$

$$d = 0.7 \text{ mm}$$

$$w = 2.7 \text{ mm}$$

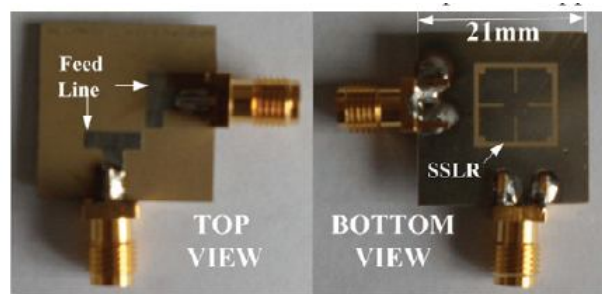


Figure 2.21: Prototype of the dual-mode SSLR filter

Simulation and experimental results are compared as shown in figure 2.22. From figure 2.22, simulated center frequency is 3.55 GHz with a wide fractional bandwidth of 3.7%. There are two transmission zeros appear at 4.09 GHz and 4.14 GHz, which can improve the upper selectivity. From the results, experiments results agree well with simulation except for a larger insertion loss of about 2.6 dB. It may due to during fabrication error and radiation loss of the slot-line resonator. (Bian Wu, Wen Su, Shou-jia Sun and Chang-Hong Liang, 2012).

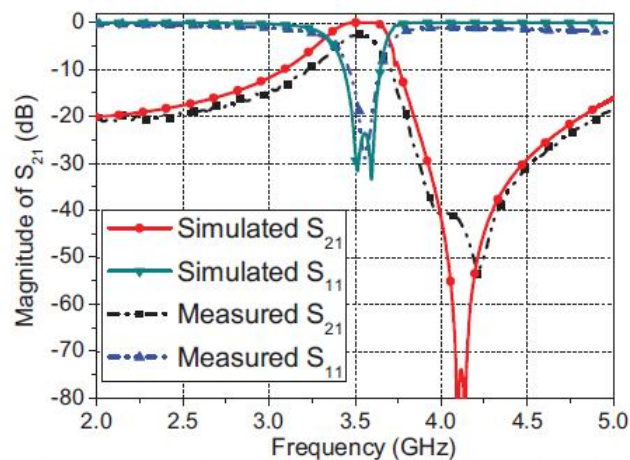


Figure 2.22: S-parameter of the simulation and experiment

An asymmetrical wideband frequency response with two upper transmission zeros are obtained by using the proposed SSLR and T-shaped feed lines. Dual-mode filter has the advantages of relatively wideband and flexible transmission zeros to realize either symmetrical or asymmetrical suppression. (Bian Wu, Wen Su, Shou-jia Sun and Chang-Hong Liang, 2012).

2.6 Introduction of Simulation Tools

During this project, we are using a lot of tools for simulation and measurement to get the proposed idea results such as High Frequency Structure Simulator (HFSS) and Microwave Office. Besides that, we also need other tools such as TX Line for calculate dimension of the strip line and Freelance Graphics software for plotting graph for writing thesis purpose. In this sub-chapter, we will introduce HFSS and Microwave office background.

2.6.1 High Frequency Structure Simulator

HFSS software is the industry-standard simulation tool for 3-D full-wave electromagnetic field simulation and is essential for the design of high-frequency and high-speed component design. HFSS offers multiple state-of the-art solver technologies based on either the proven finite element method or the well established integral equation method.

With the rapid advancement of HFSS, the analysis of the scattering matrix parameters (S, Y, Z parameters) and the visualization of the 3-D electromagnetic fields (near field and far field) can be done easily. It helps to determine the signal quality, transmission path losses, and reflection coefficients due to impedance mismatch, parasitic coupling, and radiation.

In conclusion, HFSS provides accurate results for diagnostics, prototyping and manufacturing optimisation. The use of HFSS can speed up new product development by orders of magnitude over conventional techniques. It also allows the Engineer to play with unconventional designs.

2.6.2 Microwave Office

Microwave Office is RF and microwave design software for the industry's microwave design platform with the fastest growing. Microwave Office has revolutionized the communications design world by providing users with a superior choice. Microwave Office offers unparalleled intuitiveness, powerful and innovative technologies, and unprecedented openness and interoperability, enabling integration tools for each part of the design process.

This software design suitable for high-frequency IC, PCB and module design including linear circuit simulators, non-linear circuit simulators, electromagnetic analysis tools, integrated schematic and layout, statistical design capabilities and parametric cell libraries with built-in design-rule check (DRC). AWR is a very useful tool which has a lot of pros such as faster time to market, efficiency, accurate for high performance analysis,

CHAPTER 3

BROADSIDE-COUPLED PATCH DIRECTIONAL COUPLER

3.1 Background

In directional coupler design, there are three main stages. There are simulation, fabrication and experiment stages. During these three stages, a lot of problem will occur and time is needed to obtain a better results.

3.2 Simulation Stage

In simulation stage, we are using software called HFSS (High Frequency Structure Simulator) which is in version 8. Before start design a new proposed idea, author need go through the software tutorial. Tutorial purpose is allow users familiar with the features and background of software.

After getting through HFSS tutorial, author go through few published paper and try to get the similar result as the paper results. It allow author more confident on simulation stages. Later on, few testing have been getting out for different directional coupler design.

Firstly, author need simulate on different width and length of the design stripline to match the 50Ω characteristic impedance. Width and length of the stripline can be calculated by using TX Line 2003. After meet characteristic impedance, author

required a lot of time to optimize the correct parameter. At the end, a final configuration and simulation result will be obtained.

3.3 Fabrication Stage

During this stage, author need show final simulation results to supervisor for verifying. It is because author does not need to waste the board and time to redo the design. Board material of this project is RO4003C substrate. This material has a 3.38 dielectric constant with 32 mil thickness. The board is called printed circuit board (PCB).

PCB is used to support and electrically connect electronic components using conductive pathways, track or signal traces etched from copper sheets laminated into a non-conductive substrate. Conducting layers are typically made of thin copper foil. Due to this material is not same as FR4 which they typically already laminated. So, firstly, author need coat the board with a solder mask that is in blue colour. The solder mask normally only available in green, black, white and red colour.

Next, author need transfer configuration printed on tracing paper to substrate. This is a patter transfer process. During this process, author needs done the work in a clean room which mean only yellow light are allowed. It is due to the photoresists are not sensitive to wavelength which is greater than $0.5\mu\text{m}$. Substrate only need exposed to UV light for 15 seconds.

After that, PCB need for etching process. Purpose of this process is to remove the unwanted copper and leaving only desired copper traces. After that a chemical etching is done with ferric chloride in which the board is submerged in the etching solution. This is simplest way for small-scale production, an immersion etching. Fabrication process is considered done after completing this process.

3.4 Experiment Stage

This is last stages to design a new directional coupler. Before author start to measure experimental results, author need to solder port with PCB. Purpose of this stage is for author to compare simulation and experimental results. Due to comparison, author can prove that the design can be worked in practically.

Equipment that used to measure experiment results is Rohde & Schwarz ZVB8 Vector Network Analyzer (VNA). Frequency range of this equipment is 300 kHz to 8 GHz. Equipment is design for high frequency device. In the first proposed design, directional coupler has frequency range from 2GHz to 7GHz.

After solder port, author need calibrate on the VNA machine due to different cable used has different phase of signal. VNA is able to self adjust on the S-parameters after the calibration process. The main purpose of the calibration process is to eliminate the effect of cable on the measurement and the results will more accurate. Frequency range and sweep point have to be set in order to similar to simulation result.

3.5 Broadside-coupled Patch Directional Coupler

In this subchapter, a broadside-coupled patch directional coupler was analyzing. This is a four-port with two-mode directional coupler with wide bandwidth. With this multi-port directional coupler, power splitting and network combining can be done easily. (Ferdinando Alessandri, Marco Giordano, Marco Guglielmi, Giacomo Martirano, Francesco Vitulli, May 2003). Based on design theory that has discussed on chapter 2, a four-port directional coupler with 10 dB fractional bandwidth is simulated and discussed here.

3.5.1 Configuration

A directional coupler that operates with a center frequency of 5GHz was designed. Substrate RO4003C with dielectric constant of $\epsilon_r = 2.33$ and thickness 32 mil was used in this design. Apart from that, four-port of directional coupler are designed with the characteristic impedance of 50 Ω . With the characteristic impedance of 50 Ω , directional coupler designs can easily interconnecting with other microwave systems.

This broadside-coupled patch directional coupler is design by using two substrates with the same dielectric constant and thickness. The overall dimensions of proposed design occupy and area of 50 mm x 50 mm. Proposed design formed by a rectangular and patch at the top and middle layer, where microstrip line is combining with the patch at each layer. Input and through port was lay on the top layer of the substrate. While coupler and isolation port was lay on the middle layer between two substrates. Lastly, common ground plane was form on bottom of the substrate.

With the design requirements stated above, a directional coupler was drawn by using Ansoft HFSS. Top-down view of the design is shown in figure below. Detailed parameters are given by:

$$W_1 = 14 \text{ mm}$$

$$W_2 = 31 \text{ mm}$$

$$L_1 = 5.6 \text{ mm}$$

$$L_2 = 3.3 \text{ mm}$$

$$L_3 = 3.4 \text{ mm}$$

$$L_4 = 3.1 \text{ mm}$$

$$G_1 = 3.4 \text{ mm}$$

$$G_2 = 4.0 \text{ mm}$$

$$S_1 = 50.0 \text{ mm}$$

$$S_2 = 50.0 \text{ mm}$$

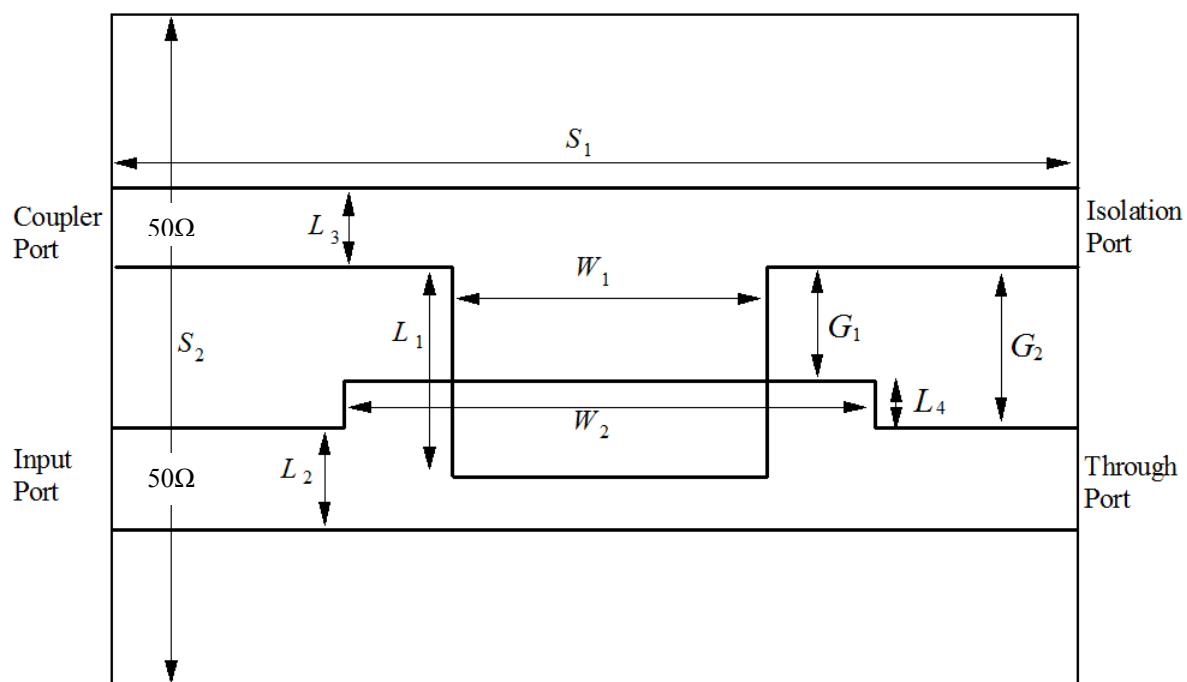
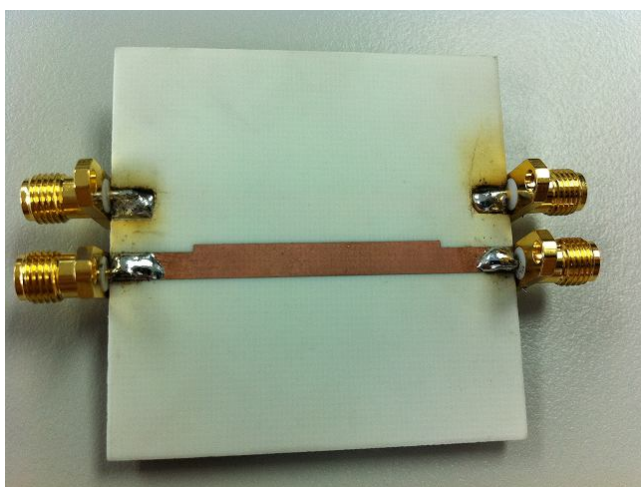
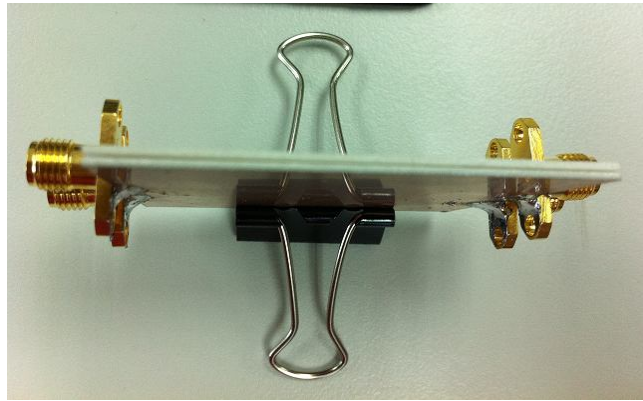


Figure 3.1: Dimension of broadside-coupled patch directional coupler



(a)



(b)



(c)

Figure 3.2: Prototype of the proposed broadside-coupled patch directional coupler.

(a) Top-down view, (b) Side view, (c) Bottom view

3.5.2 Result and Discussion

In order to test performances of directional coupler design, experiments were carried out by using Rohde and Schwarz ZVB8 VNA. Amplitude of the proposed directional coupler was compared. Figure 3.3 shows magnitude response for the simulation and experimental of broadside-coupled patch directional coupler.

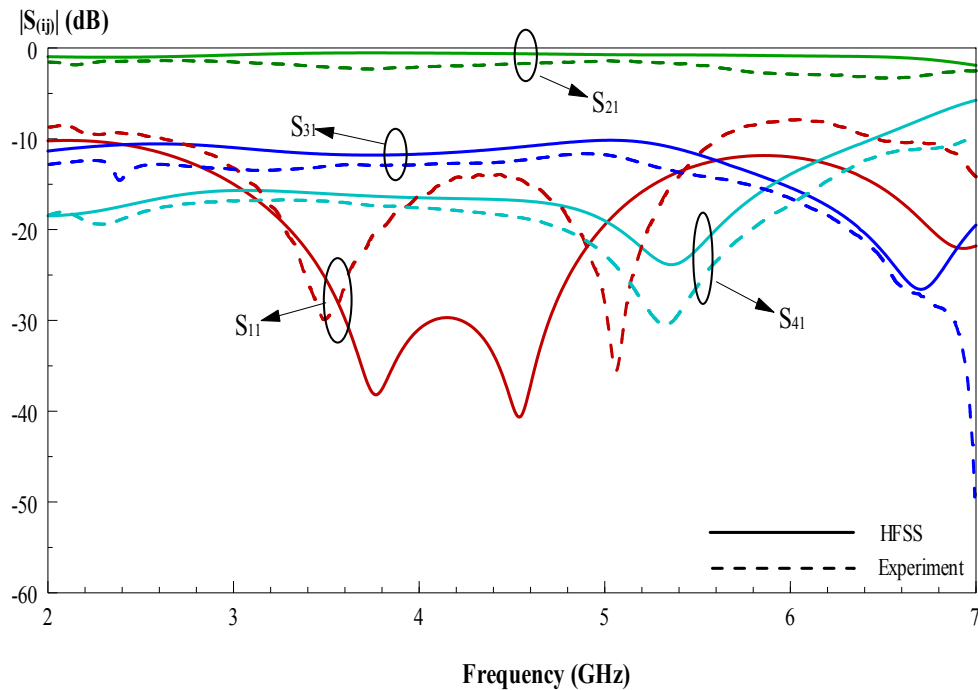


Figure 3.3: Magnitude response of broadside-coupled patch directional coupler

Based on figure above, it is a two-mode directional coupler can be realised in the proposed design. Experimental result was proven well with the simulation result. From simulation and experimental result, a 10 dB flat coupling can be achieved in frequency range of 4 to 5.5 GHz for simulation and 3.5 to 5.2 GHz for experimental result. Simulation gives a total bandwidth of 1.5 GHz and experimental gives a total bandwidth of 2 GHz.

Besides that, there are two poles contributing to wideband performance of the directional coupler design. First pole locate at 3.6 GHz and second pole locate at 4.7 GHz for simulation result. While for experimental result, first pole locate at 3.5 GHz and second pole at 5.1 GHz.

From Figure 3.3, center frequency and fractional bandwidth can be calculate and form in Table 3.1 which shows comparison of the experimental and simulation results. Equation center frequency, fractional bandwidth and difference between simulation and experimental percentages as following:

$$f_c = \left(\frac{f_H + f_L}{2} \right)$$

$$\text{Fractional Bandwidth, FBW} = \left(\frac{f_H - f_L}{f_c} \right)$$

$$\text{Area, } \bar{e} = \left(\frac{f_{c(\text{exp})} - f_{c(\text{sim})}}{f_{c(\text{exp})}} \right) \times 100\%$$

For the simulation calculation shown as following:

$$f_c = \left(\frac{5.5 + 4.0}{2} \right) = 4.75 \text{ GHz}$$

$$\text{Fractional Bandwidth, FBW} = \left(\frac{5.5 - 4.0}{4.75} \right) \times 100\% = 31.60\%$$

For the experiment calculation shown as following:

$$f_c = \left(\frac{5.2 + 3.2}{2} \right) = 4.35 \text{ GHz}$$

$$\text{Fractional Bandwidth, FBW} = \left(\frac{5.2 - 3.2}{4.35} \right) \times 100\% = 41.40\%$$

Percentages difference between simulation and experiment:

$$\text{Area, } \bar{e} = \left(\frac{4.35 - 4.75}{4.35} \right) \times 100\% = 9.2\%$$

Table 3.1: Comparison of the experimental and simulation results

	HFSS Simulation	Experiment
f_L (GHz), f_H (GHz)	4.00, 5.50	3.20, 5.20
f_c (GHz)	4.75	4.35
Fractional Bandwidth (%)	31.60	41.40

Fractional bandwidth difference between experimental and simulation is 9.2% which is less than 10%. The difference between experimental and simulated may due to alignment of two layers. That is very difficult to make exact alignment of two layer same as alignment in the simulation part.

3.5.3 Parametric Analysis

In this subchapter, parametric analysis will be analyzed. We needs to simulate proposed directional coupler using modified parameter with the same frequency range in order to ease the comparison. It aims is to prove values selected in configuration are able to perform better compare with other values. Different values of design dimension are used to be simulated and results are discussed in this section.

Analysis 1

- Parameter : W_1
- Optimum value : 14.0 mm
- Step-down value : 13.8 mm
- Step-up value : 14.2 mm

Result:

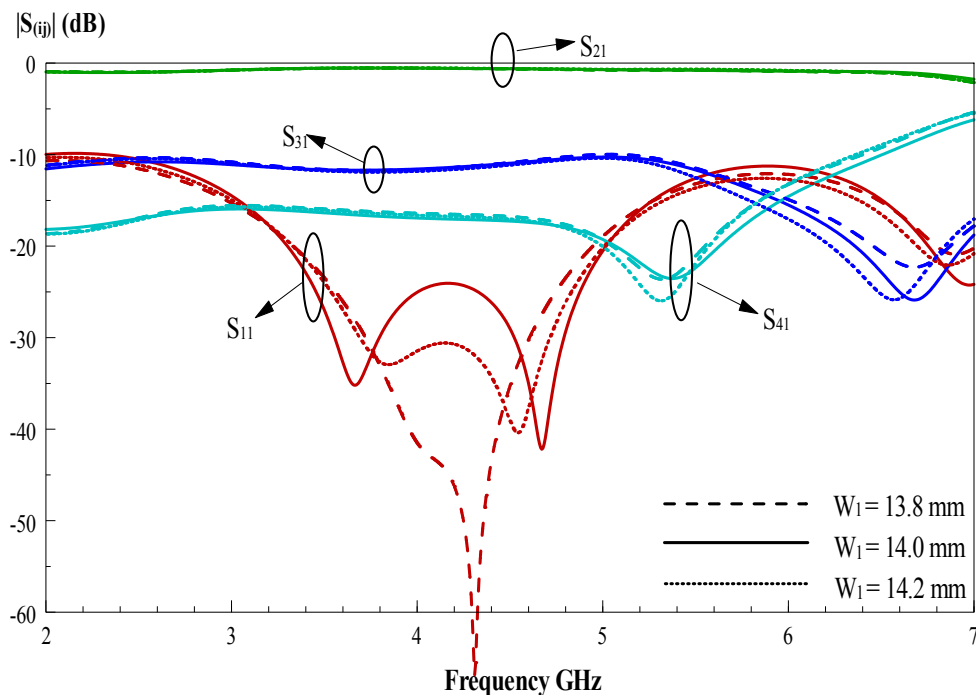


Figure 3.4: Effect of width W_1 on the proposed directional coupler

Parameter W_1 does not affect simulation results much on the proposed directional coupler. It only slightly affects the position poles on proposed directional coupler. According to Figure 3.4, optimal value of W_1 can give the best reflection coefficient S_{11} with a matching level below -25 dB across the operating frequency band.

Analysis 2

- Parameter : W_2
- Optimum value : 31.0 mm
- Step-down value : 30.8 mm
- Step-up value : 31.2 mm

Result:

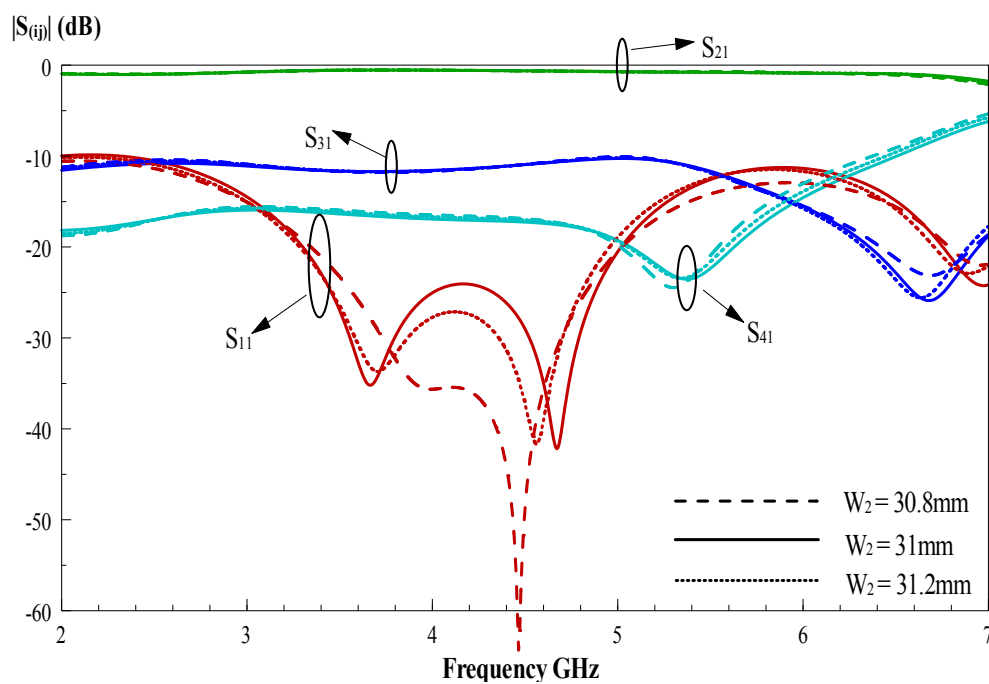


Figure 3.5: Effect of width W_2 on the proposed directional coupler

Parameter W_2 also does not affect the simulation result much. It also slightly affects position poles on proposed directional coupler. Besides that, it is same as parameter W_1 which it can give the best reflection coefficient S_{11} with a matching level below -25 dB across the operating frequency band.

Analysis 3

- Parameter : L_1
- Optimum value : 5.6 mm
- Step-down value : 5.1 mm
- Step-up value : 6.1 mm

Result:

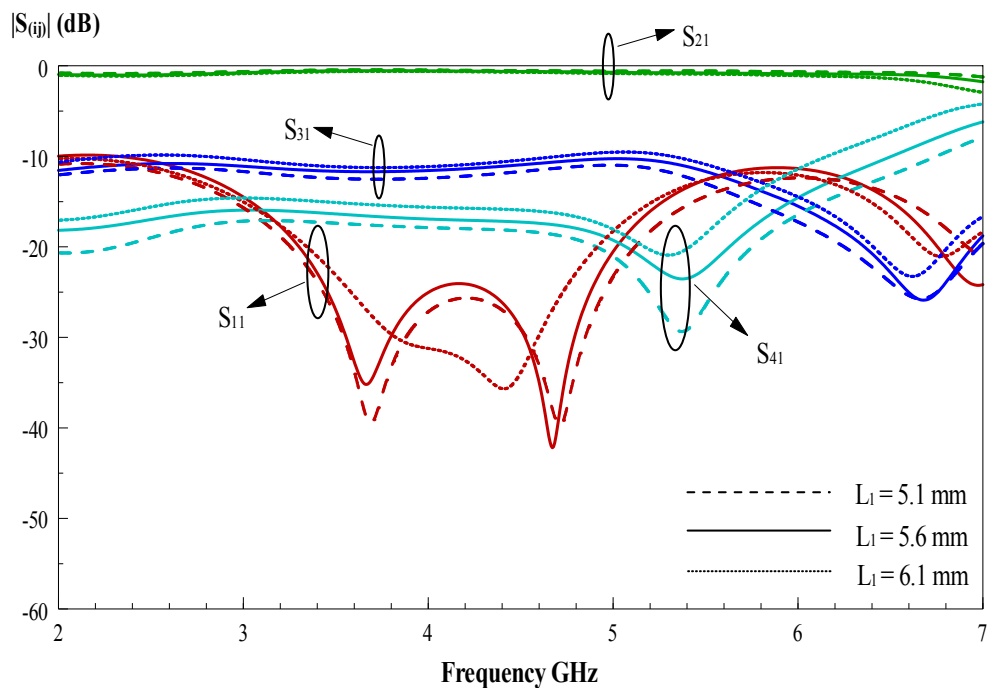


Figure 3.6: Effect of length L_1 on the proposed directional coupler

When the length of center patch getting larger, the matching at port 1 will also changes. Refer to Figure 3.6, matching level is maintained below -25 dB at optimum gap of 5.60 mm. This is important to ensure that the input signal is not reflected back to input port.

Analysis 4

- Parameter : L_2
- Optimum value : 3.3 mm
- Step-down value : 3.1 mm
- Step-up value : 3.5 mm

Result:

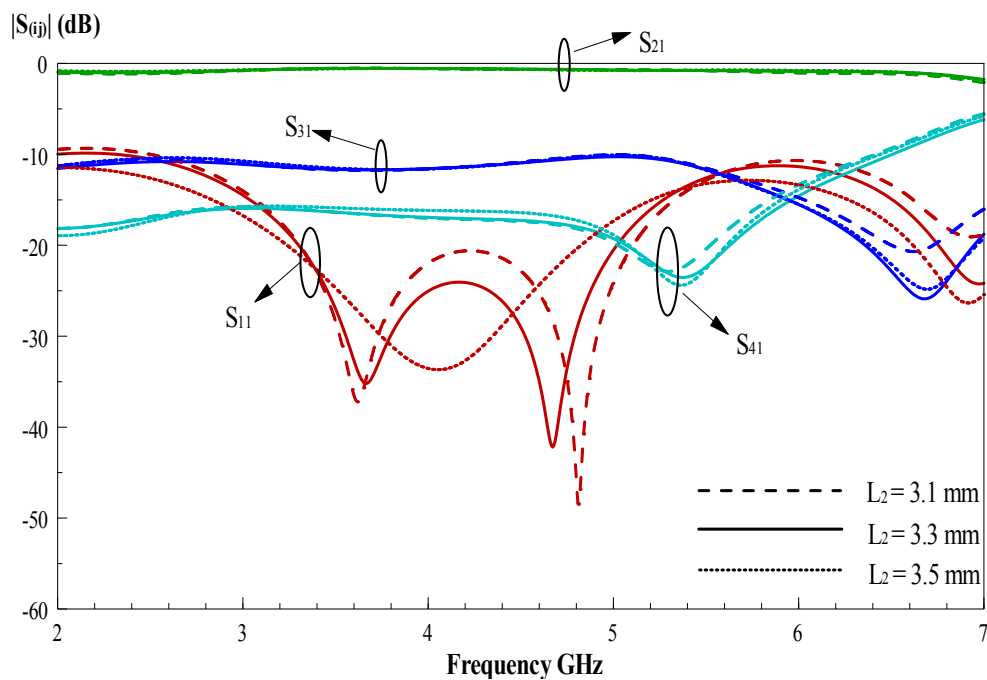


Figure 3.7: Effect of length L_2 on the proposed directional coupler

It is same as when the length of top patch larger and the matching at port 1 will also change. But it does not affect the coupling port. When the length of top patch equal to 3.5 mm, the matching at port 1 will become one-mode. It also does not affect the other three ports.

Analysis 5

- Parameter : L_3
- Optimum value : 3.1 mm
- Step-down value : 2.9 mm
- Step-up value : 3.3 mm

Result:

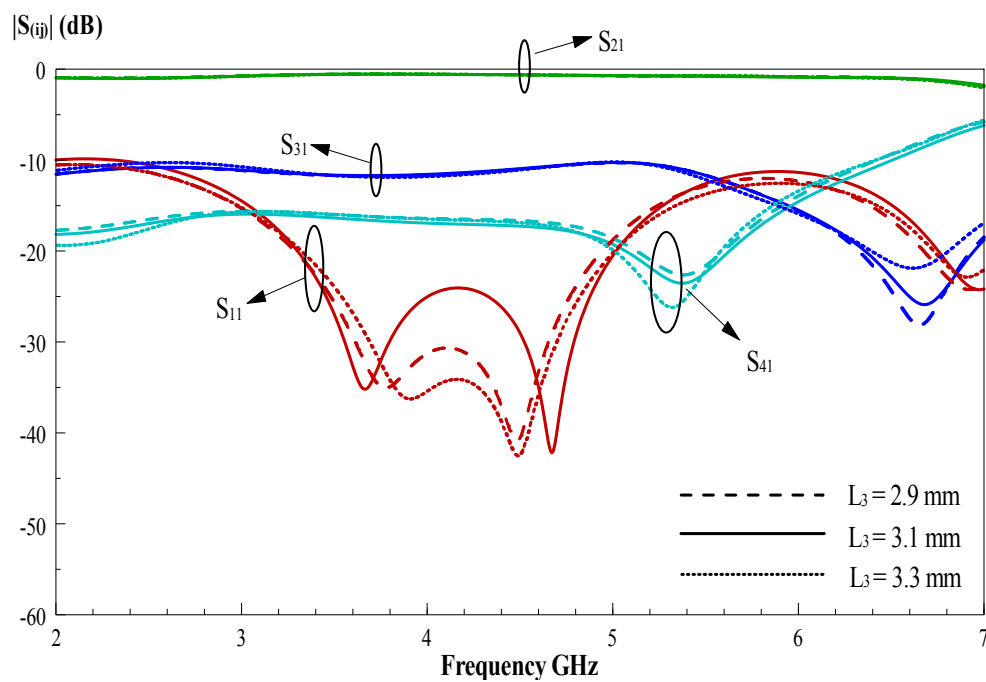


Figure 3.8: Effect of length L_3 on the proposed directional coupler

Length L_3 has no significant effect on the coupling level. However, it causes the matching to vary. Obviously, it is much better when L_3 is equal to the optimum value. It can be maintained well below -25 dB.

Analysis 6

- Parameter : L_4
- Optimum value : 0.9 mm
- Step-down value : 0.7 mm
- Step-up value : 1.1 mm

Result:

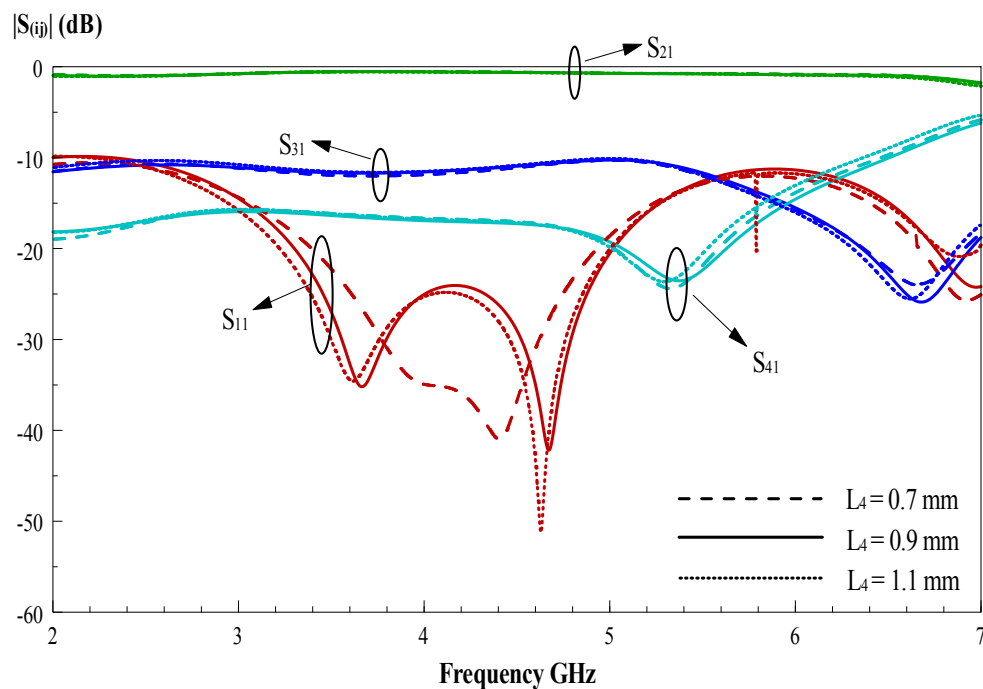


Figure 3.9: Effect of length L_4 on the proposed directional coupler

The input of proposed directional coupler is affected when the length L_4 changes. When L_4 is decreased, the first pole of the directional coupler shifts higher. Also, it moves to combine with the second pole. The through port keep remain approximate 0 dB. That mean, most of the signal passed through the device and the return loss is weak.

Analysis 7

- Parameter : G_1
- Optimum value : 3.4 mm
- Step-down value : 2.4 mm
- Step-up value : 4.4 mm

Result:

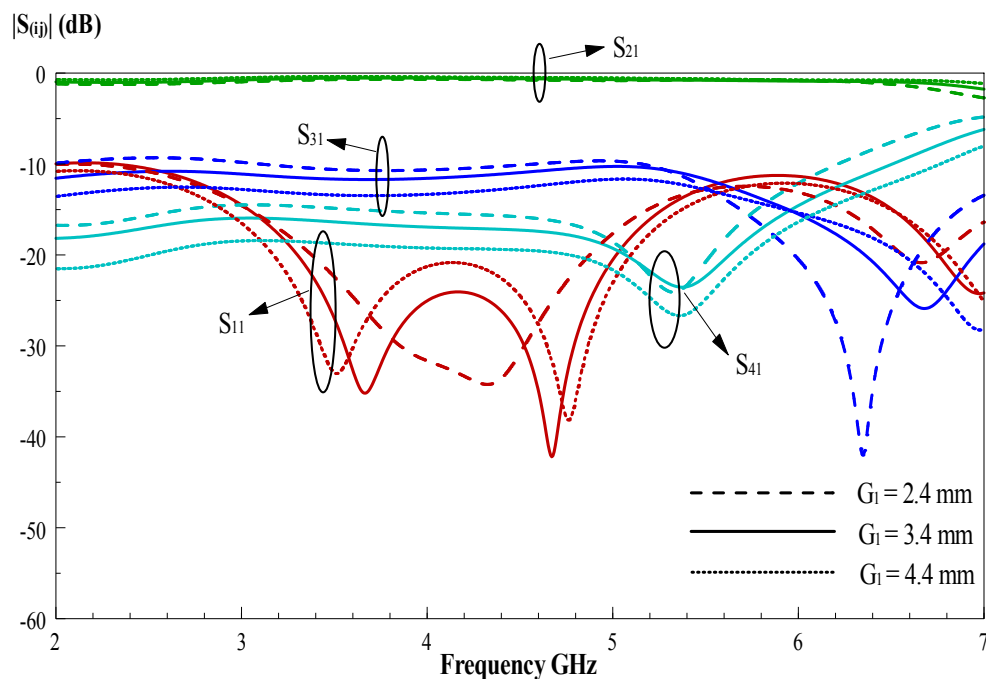


Figure 3.10: Effect of gap G_1 on the proposed directional coupler

As for the coupled-line directional coupler, the gap between the top patch and middle stripline play an important role in the determination of the desired coupling level of the directional coupler. When the gap G_1 is stepped down to 2.4 mm, the matching level becomes poorer while the coupling level stays below 10 ± 1 dB. In another case, G_1 is stepped up to 4.4 mm, the coupling level is only about -14 ± 1 dB, which is not the desired value. The optimum gap size for G_1 is 3.4 mm.

Analysis 8

- Parameter : G_2
- Optimum value : $G_2 = 4.0$ mm
- Step-down value : $G_2 = 4.3$ mm
- Step-up value : $G_2 = 4.6$ mm

Result:

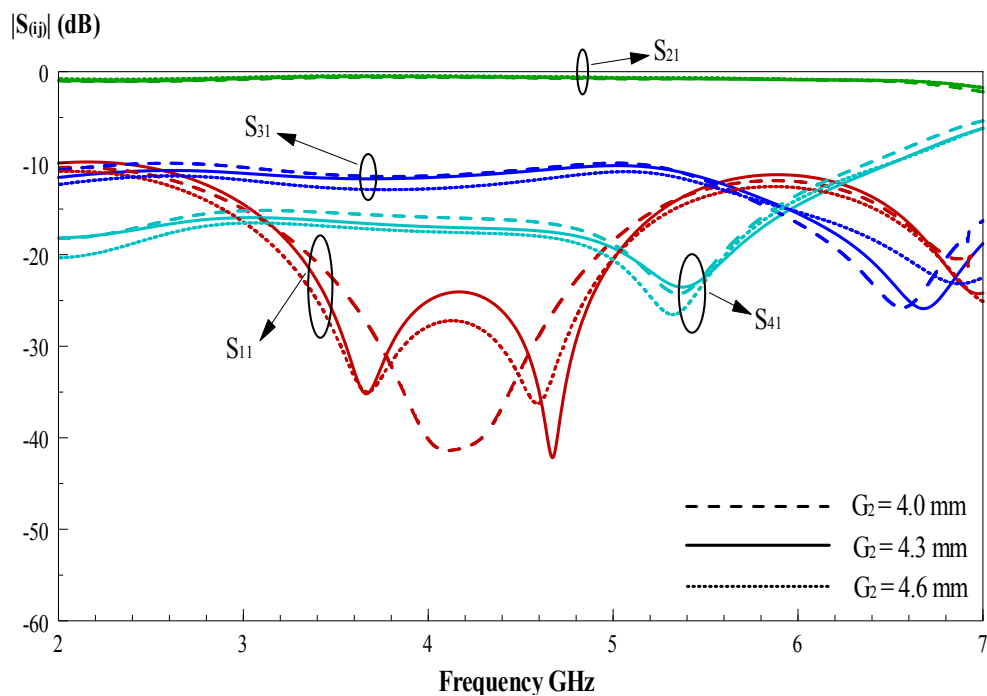


Figure 3.11: Effect of gap G_2 on the proposed directional coupler

By controlling the gap G_2 , the coupling level of the proposed directional coupler can be adjusted. When the gap size is 4.0 mm, the matching at port 1 has combine first pole and second pole. As a result, the received power at port 3 is lesser able couple through the coupled lines. If the gap G_2 increased to 4.6 mm, the difference between S_{21} and S_{31} falls out of range of 10 ± 1 dB. The gap G_2 is designed as 4.3 mm to achieve a constant coupling of 10 ± 1 dB at the desired operating frequencies.

Analysis 9

- Parameter : S_1
- Optimum value : 50 mm
- Step-down value : 40 mm
- Step-up value : 60 mm

Result:

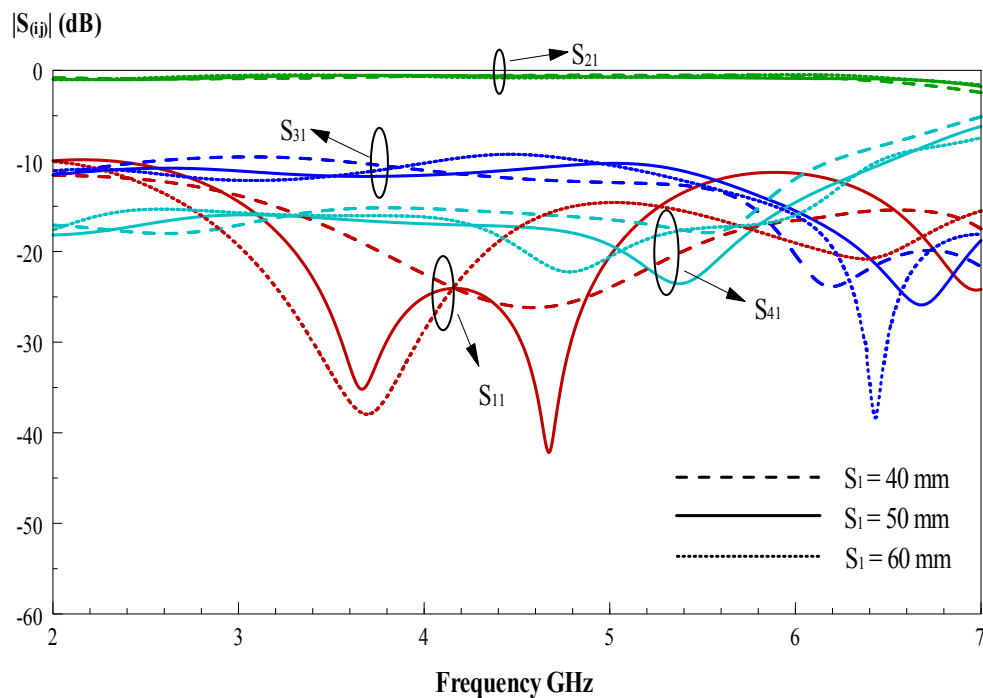


Figure 3.12: Effect of substrate S_1 on the proposed directional coupler

When the substrate length is not optimum value, the matching port was totally changed and the return loss was so high. Apart from that, the bandwidth of coupling port was less than 10 ± 1 dB. It may be due to the stripline of two layers becoming shorter, the impedance matching was reduced.

Analysis 10

- Parameter : S_2
- Optimum value : 50 mm
- Step-down value : 40 mm
- Step-up value : 60 mm

Result:

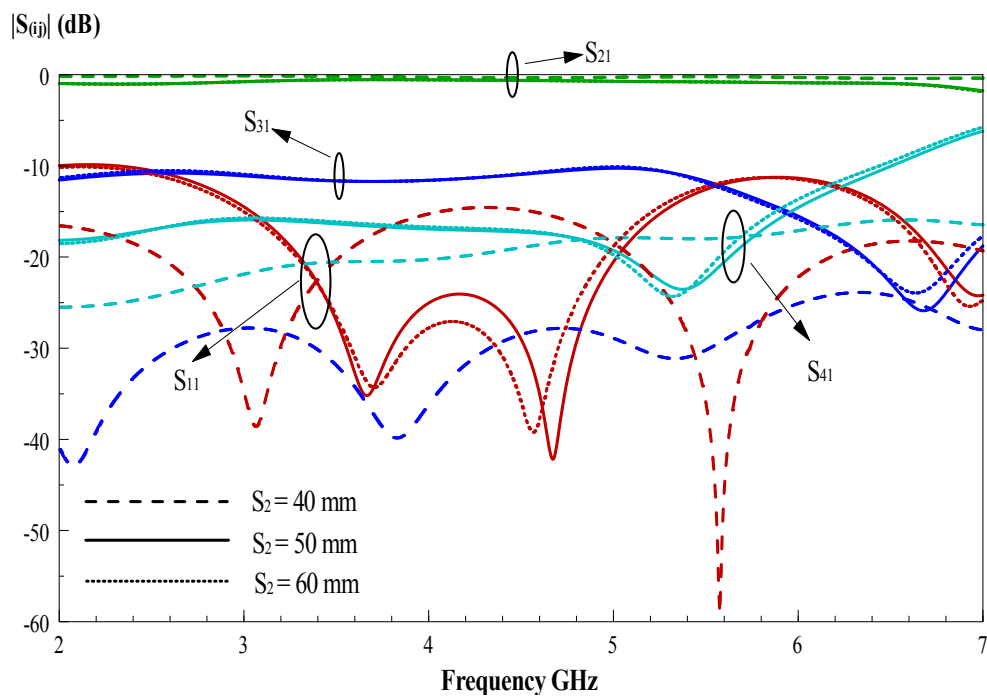


Figure 3.13: Effect of substrate S_2 on the proposed directional coupler

The coupling level was totally out of the range when S_2 set to 40 mm. The fractional bandwidth cannot maintain in the range of 10 ± 1 dB. Besides that, the position of the two poles was shift to 3.1 GHz and 5.6 GHz. But when the S_2 set to 60 mm, the coupling level does not affect by the changes.

Analysis 11

- Parameter : $S_1 = S_2$
- Optimum value : 50 mm
- Step-down value : 40 mm
- Step-up value : 60 mm

Result:

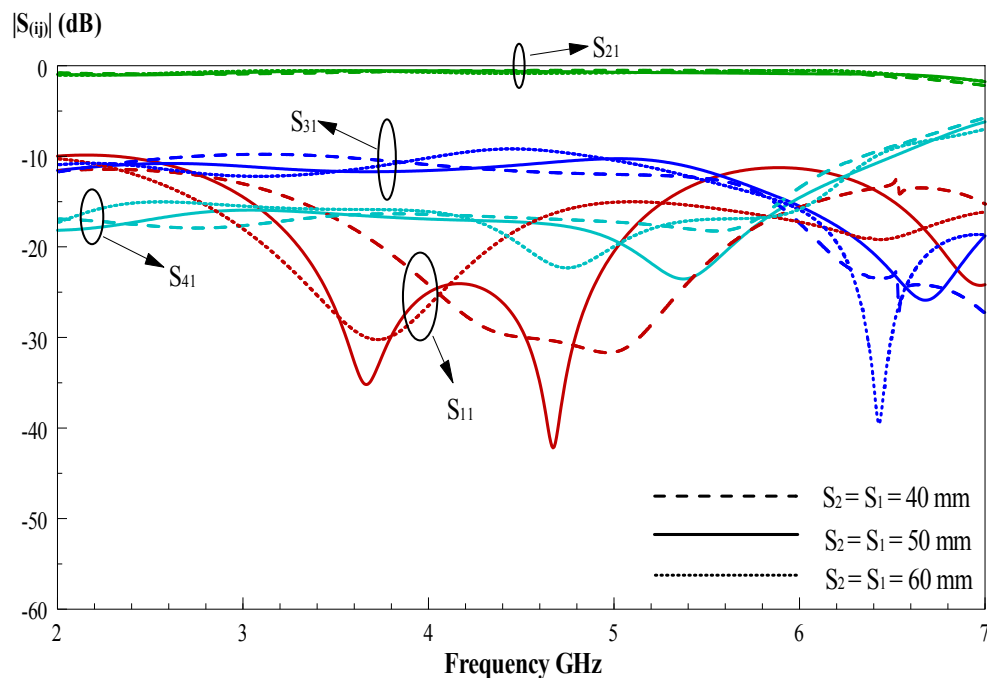


Figure 3.14: Effect of substrate size S_1 and S_2 on the proposed directional coupler

In this analysis, we are tried to compare the difference by changing two parameters together. For example, the substrate sizes reduce to 40 mm x 40 mm. From the figure above, the matching at port 1 are going to combine the first pole with second pole. On the other hand, when the substrate size is enlarge to 60 mm x 60 mm the second pole was far away from the optimum value.

Analysis 12

- Parameter : H_1
- Optimum value : 0.8128 mm
- Step-up value : 1.5240 mm

Result:

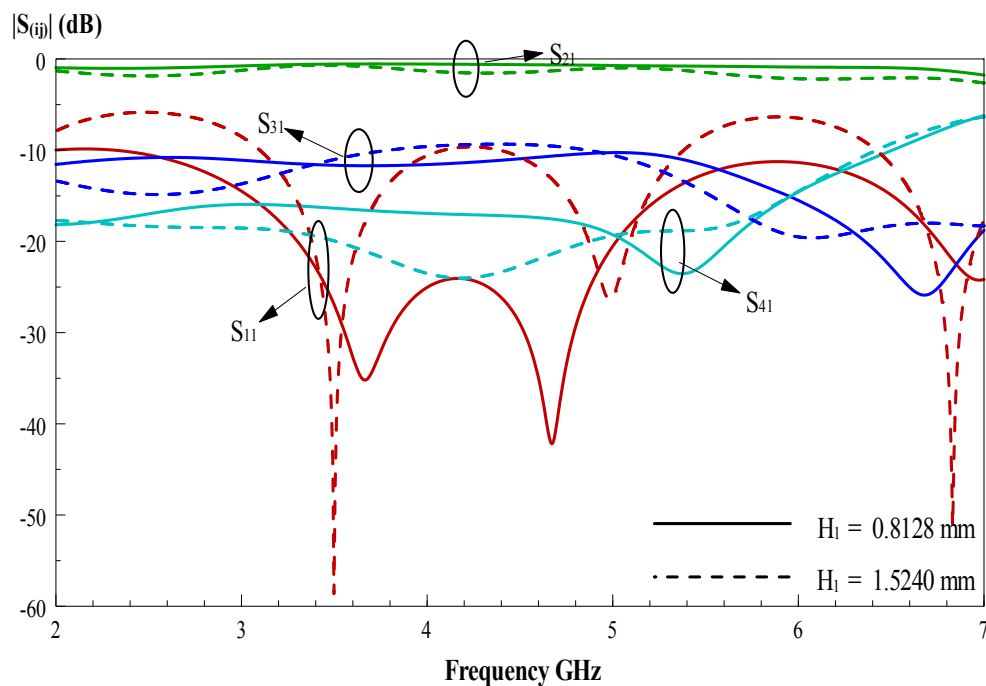


Figure 3.15: Effect of substrate thickness H_1 on the proposed directional coupler

In this analysis, we are using the same dielectric constant with different thickness. The substrate that we compare is a RO4003C with thickness 32 mil and 60 mil which is 0.8128 mm and 1.5240 mm. It is better if the matching at port 1 was less than -10 dB. By using the 60 mil thickness, the coupling level was higher than 10 ± 1 dB. So the optimum value is chosen to be 0.8128.

Analysis 13

- Parameter : L_2, L_3
- Optimum value : $L_2 = 3.3 \text{ mm}, L_3 = 3.1 \text{ mm}$
- Step-down value : $L_2 = L_3 = 2.8 \text{ mm}$
- Step-up value : $L_2 = L_3 = 3.8 \text{ mm}$

Result:

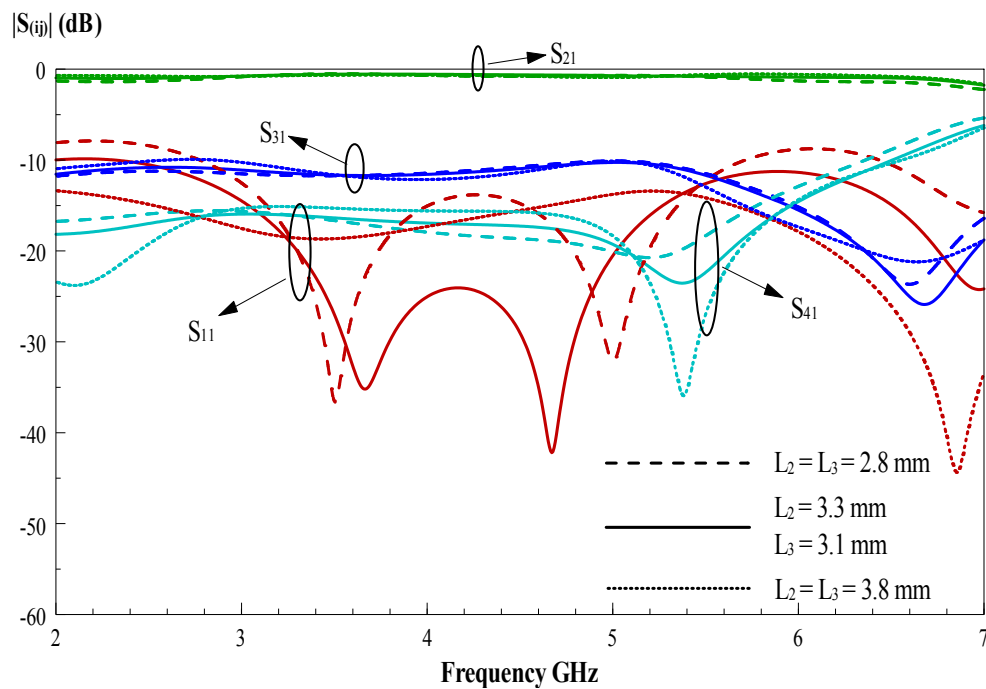


Figure 3.16: Effect of length L_2 and L_3 on the proposed directional coupler

With reference to the amplitude response shown in Figure 3.16, we can clearly see that the gap g_2 affects the input port of the proposed directional coupler. When L_2 and L_3 are set as 2.8 mm, the poles were difference with the optimum choice. When L_2 and L_3 are stepped up to 3.8 mm, the matching level was not maintained at the 25dB. In this case, the value of L_2 and L_3 is chosen to be 3.3 mm and 3.1 mm.

Analysis 14

- Parameter : L_1, L_4
- Optimum value : $L_1 = 5.6 \text{ mm}, L_4 = 0.9 \text{ mm}$
- Step-down value : $L_1 = L_4 = 5.2 \text{ mm}$
- Step-up value : $L_1 = L_4 = 6.0 \text{ mm}$

Result:

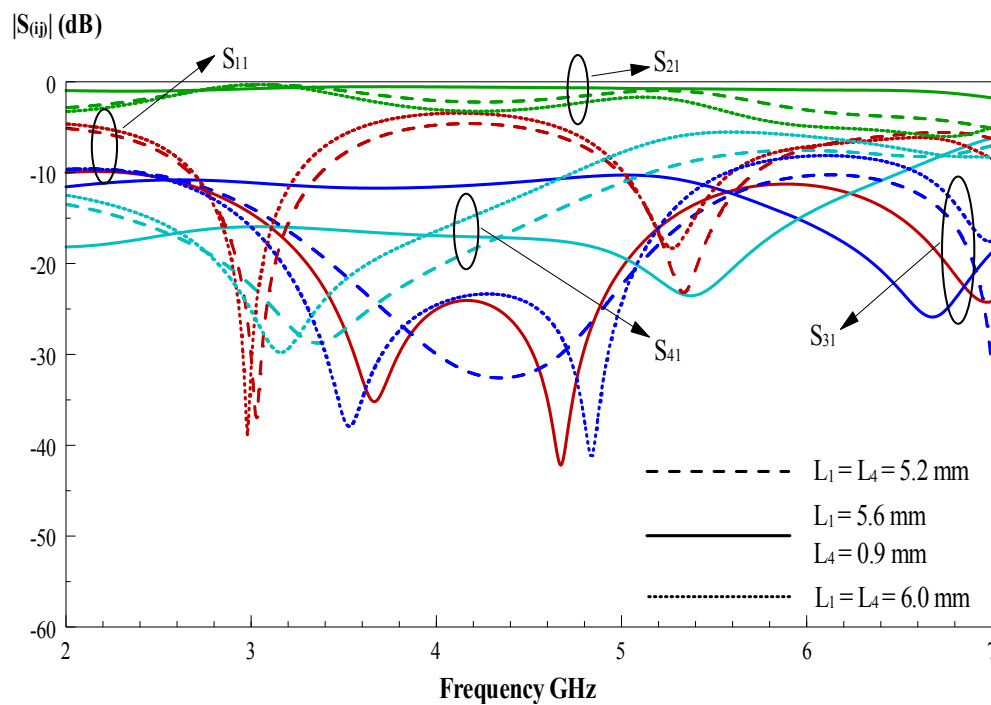


Figure 3.17: Effect of length L_1 and L_4 on the proposed directional coupler

When the length of the middle and top patch are equal, the characteristic impedance of the top patch is no longer 50Ω . So, most of the signal cannot pass through the device and the coupling level cannot maintain on $10 \pm 1 \text{ dB}$. There is a high return loss and low insertion loss.

Analysis 15

- Parameter : W_1, W_2
- Optimum value : $W_1 = 14.0 \text{ mm}, W_2 = 31.0 \text{ mm}$
- Step-down value : $W_1 = W_2 = 12.0 \text{ mm}$
- Step-up value : $W_1 = W_2 = 16.0 \text{ mm}$

Result:

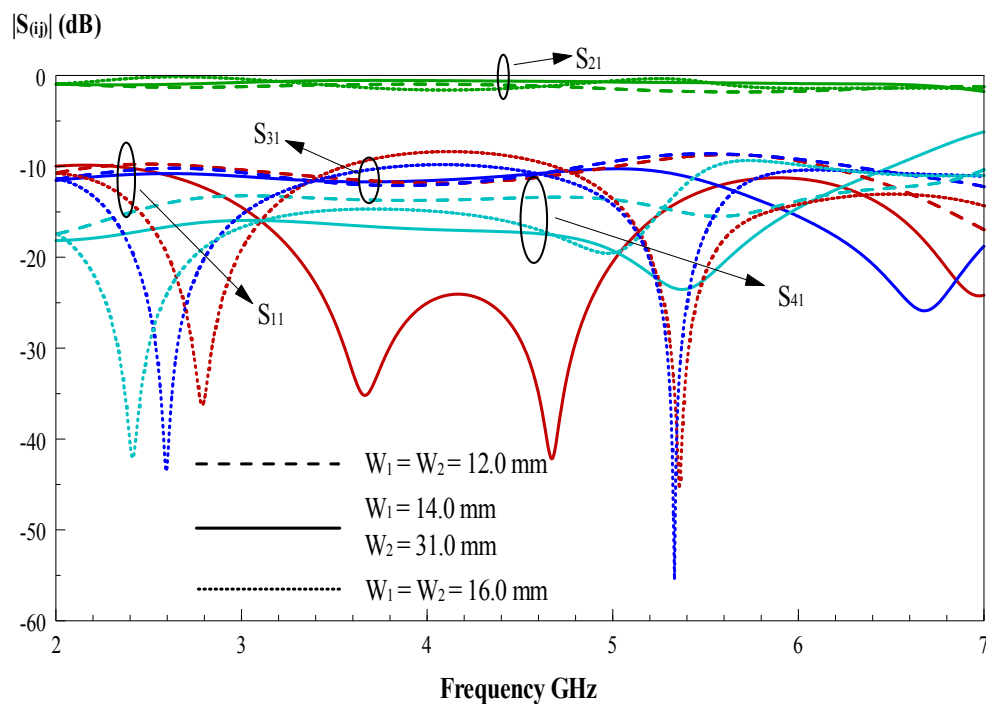


Figure 3.18: Effect of width W_1 and W_2 on the proposed directional coupler

The situation of this case is similar to previous. The flat coupling fails to maintain at $10 \pm 1 \text{ dB}$ if the value of W_1 and W_2 changes. Apart from that, the impedance matching level becomes poorer, causing the bandwidth of the proposed directional coupler to reduce.

Analysis 16

- Parameter : G_1, G_2
- Optimum value : $G_1 = 3.4 \text{ mm}, G_2 = 4.3 \text{ mm}$
- Step-down value : $G_1 = 2.4 \text{ mm}, G_2 = 3.3 \text{ mm}$
- Step-up value : $G_1 = 4.4 \text{ mm}, G_2 = 5.3 \text{ mm}$

Result:

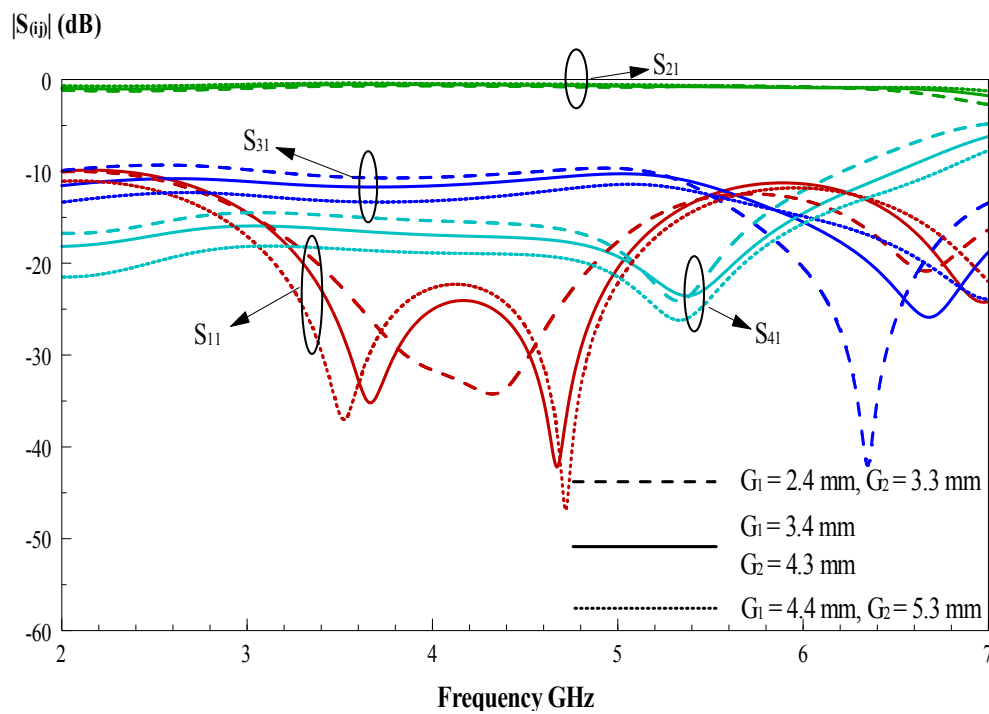


Figure 3.19: Effect of gap G_1 and G_2 on the proposed directional coupler

Figure 3.19 shows the effect of G_1 and G_2 on the magnitude response. It can be seen that flat coupling fails to maintain at $10 \pm 1 \text{ dB}$ if the value of G_1 and G_2 changes. Apart from that, the first pole was combining together with second pole when the G_1 and G_2 set to 5.3 mm.

CHAPTER 4

TRAVELLING-WAVE SECTORIAL SLOT RESONATOR

4.1 Background

Microwave resonators are widely used in a variety of application, including filters, oscillator, frequency meters and tuned amplifiers. Operations of microwave resonators are very similar to lumped-element resonators of circuit theory. Various implementations of resonators at microwave frequencies distributed elements such as transmission lines, rectangular and circular waveguide, and dielectric cavities. In this chapter, we will discuss proposed resonator which is a travelling-wave slot resonator.

A resonator is a device or system that exhibits resonance or resonant behaviour. It naturally oscillates at resonant frequencies, with greater amplitude than at others. The oscillations in a resonator can be either electromagnetic or mechanical. Resonators are used to either generate waves of specific frequencies or to select specific frequencies from a signal. A microwave resonator can usually either a series or parallel RLC lumped-element equivalent circuit.

4.1.1 Series RLC Resonator

Figure 4.1 shows the series RLC resonator circuit.

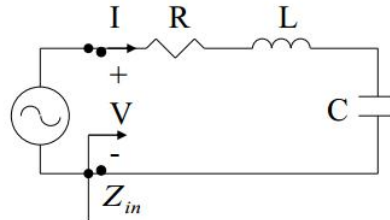


Figure 4.1: Series RLC resonator circuit

Power dissipated by the resistor, R:

$$P_{loss} = \frac{1}{2} |I|^2 R$$

Average magnetic energy stored in the inductor:

$$W_m = \frac{1}{4} |I|^2 L$$

Average electric energy stored in the capacitor, C:

$$W_e = \frac{1}{4} |V_c|^2 C = \frac{1}{4} |I|^2 \frac{1}{\omega^2 C}$$

Complex power delivered to the resonator is

$$P_{in} = P_{loss} + 2j\omega(W_m - W_e)$$

Input of a series RLC lumped-element resonant circuit as following equation:

$$Z_{in} = \frac{2P_{in}}{|I|^2} = \frac{P_{loss} + 2j\omega(W_m - W_e)}{|I|^2/2}$$

Quality factor and bandwidth:

$$Q(\omega) = \omega \frac{\text{average energy stored}}{\text{energy loss/second}} = \omega \frac{W_m + W_e}{P_{loss}}$$

$$BW = \frac{1}{Q}$$

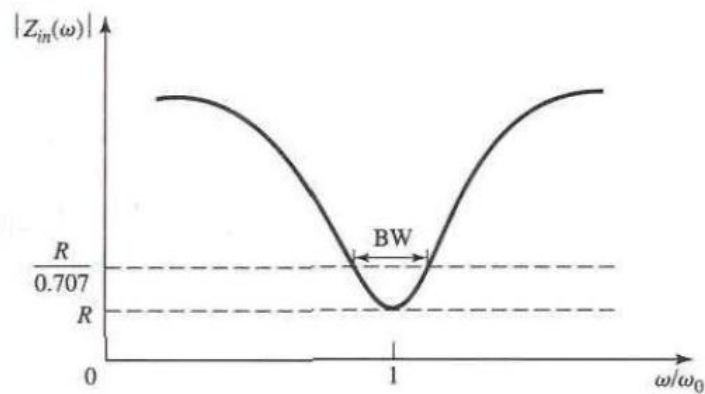


Figure 4.2: Input impedance magnitude of a series RLC resonator

4.1.2 Parallel RLC Resonator

Parallel RLC resonant circuit as shown in figure 4.3 is the dual of the series RLC circuit. The power dissipated by the resistor, R :

$$P_{loss} = \frac{1}{2} \frac{|V|^2}{R}$$

Average electric energy stored in the capacitor, C :

$$W_e = \frac{1}{4} |V_e|^2 C$$

Average magnetic energy stored in the inductor:

$$W_m = \frac{1}{4} |I_L|^2 L = \frac{1}{4} |V|^2 \frac{1}{\omega^2 L}$$

The I_L is the current pass through the inductor. Then complex power delivered to the resonator is

$$P_{in} = P_{loss} + 2j\omega(W_m - W_e)$$

Similarly, the input of a series RLC lumped-element resonant circuit as following equation:

$$Z_{in} = \frac{2P_{in}}{|I|^2} = \frac{P_{loss} + 2j\omega(W_m - W_e)}{|I|^2/2}$$

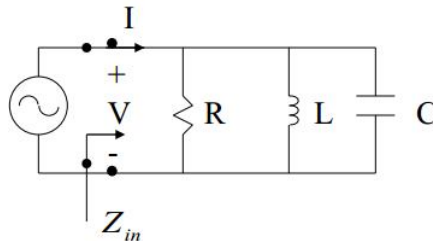


Figure 4.3: Parallel RLC resonant circuit

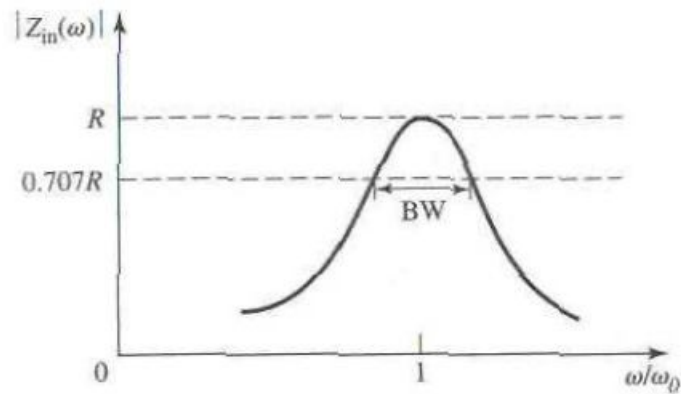


Figure 4.4: The input impedance magnitude of the parallel RLC resonator.

4.2 Configuration

Configuration travelling-wave sectorial slot resonator design shown as Figure 4.5. It is a RO4003C substrate with thickness of 32 mil and dielectric constant of 3.38. Design has two substrates with the same material. The first slot was laid on top layer of the first substrate. The second slot lay on bottom layer of second substrate. Dimension details of the configuration and results will be discussed in this subchapter. The design is still under optimizing the exact parameters.

Figure 4.5 shows proposed resonator configuration which is still under optimizing. The figure included bottom-layer, top-layer and middle-layer structure. From the configuration, author can know that signals are pass by input port (port 1) to output port (port 2 and port 3) through the slot in middle layer. Dimension of resonator as following:

$$\epsilon_r = 3.38$$

$$H_1 = 0.8128 \text{ mm} / 32 \text{ mil}$$

$$W_1 = 1.75 \text{ mm}$$

$$W_2 = W_3 = 1.7 \text{ mm}$$

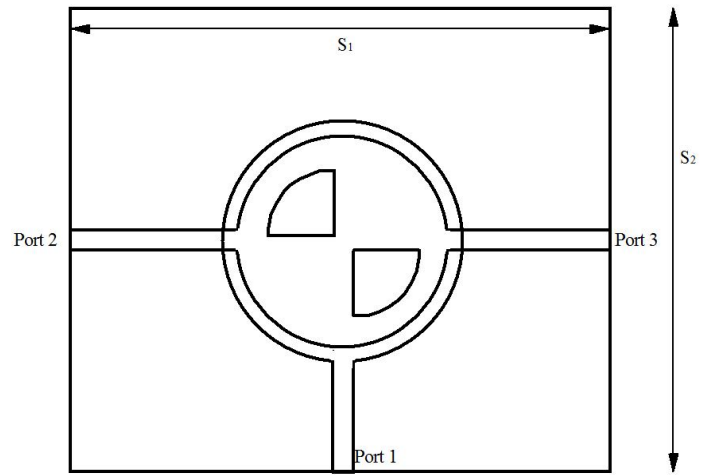
$$R_1 = 14 \text{ mm}$$

$$R_2 = 12 \text{ mm}$$

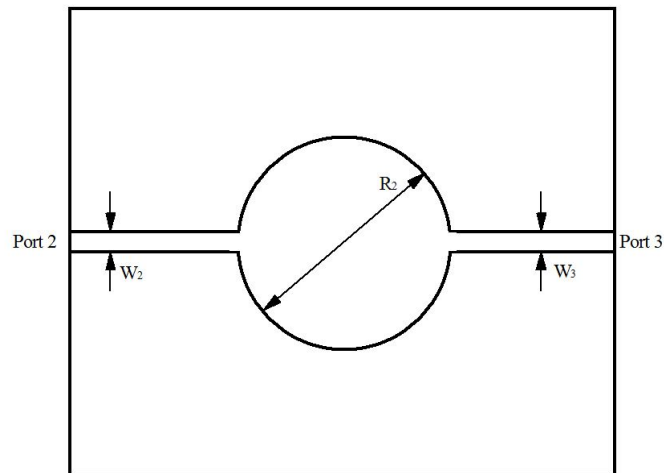
$$R_3 = 8 \text{ mm}$$

$$S_1 = S_2 = 70 \text{ mm}$$

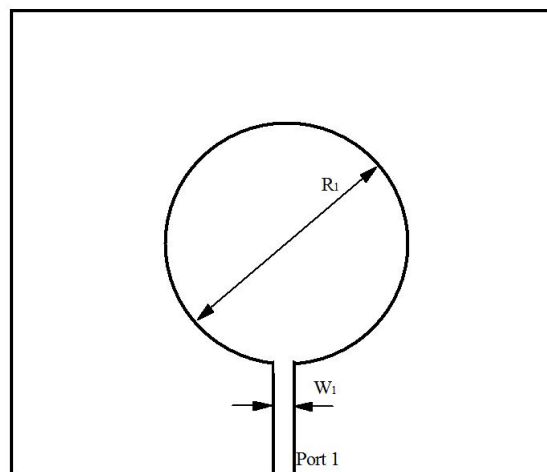
$$G_1 = G_2 = 0.5 \text{ mm}$$



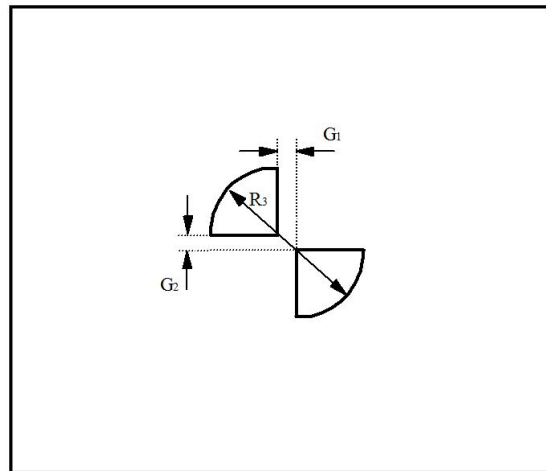
(a)



(b)



(c)



(d)

Figure 4.5: Configuration of the proposed resonator (a) Top-down view (b) Bottom-layer structure (c) top-layer structure (d) middle-layer structure

4.3 Results and Discussion

Figure 4.6 shows S-parameter of the proposed resonator. This S-parameter is a reference for comparing the parameter analysis due to the design is still under optimizing stages. The frequency should move to 3 GHz. It is because most of the communication system is at 3 GHz.

From below figure, input impedance is lower than 12 dB which means signal pass through the device is higher and the return loss is low. It is a two-mode resonator which the poles are at 3.05 GHz and 3.14 GHz with center frequency at 3.1 GHz. For this design, author cannot get experimental results due to run out of time. Another problem is center frequency need move to 3 GHz.

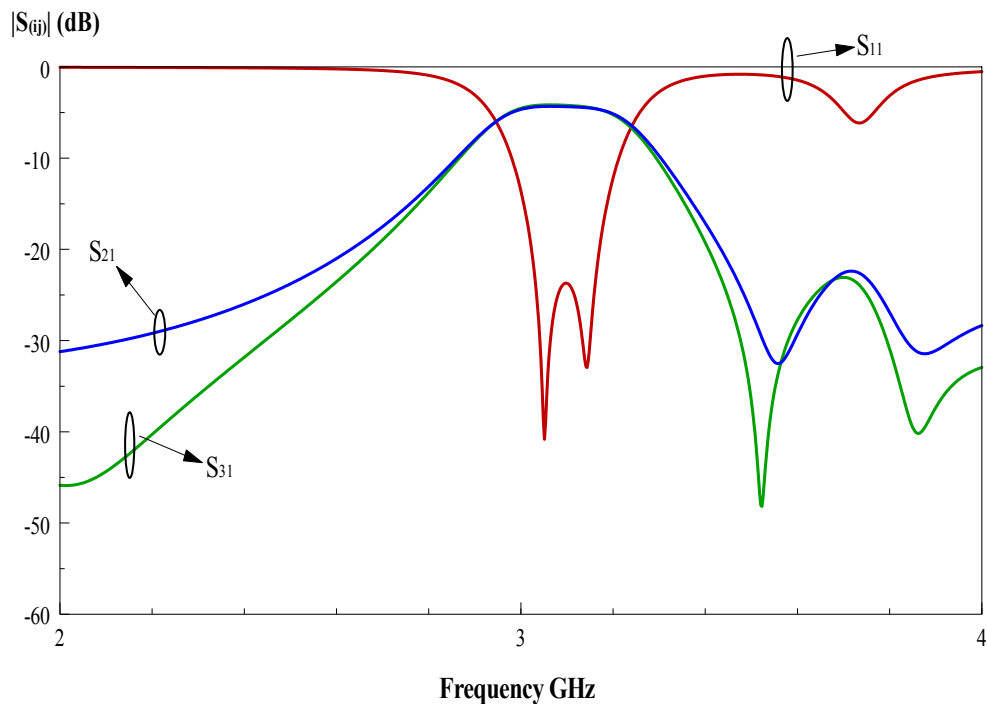


Figure 4.6: S-parameter of the proposed resonator

4.4 Parametric Analysis

All the design parameters were analyzed using HFSS to study the effects. Design considerations and issues of each parameter will be discussed here. Proposed resonator is simulated by using modified parameter with the same frequency range in order to ease the comparison. It aims to prove that values selected in configuration are able to perform better compare with other values.

Analysis 1

- Parameter : R_1
- Optimum value : $R_1 = 13$ mm
- Step-down value : $R_1 = 12$ mm
- Step-up value : $R_1 = 14$ mm

Result:

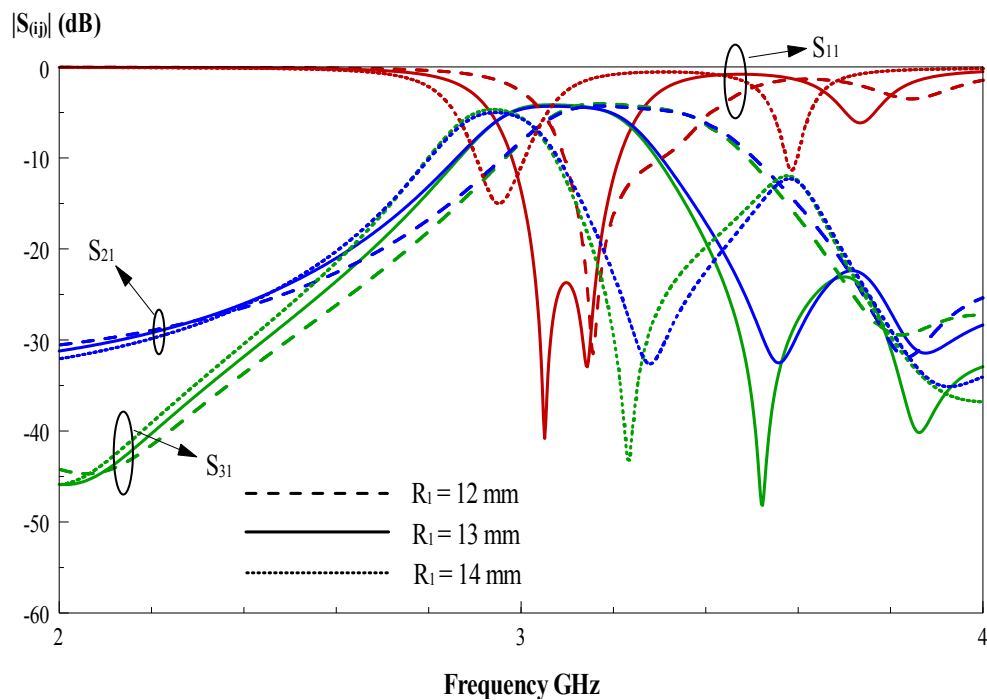


Figure 4.7: Effect of radius R_1 on the proposed resonator

From the figure above, the two-mode of the input impedance was combined when the radius of the first patch changes to 12 mm or 14 mm. Besides that, the frequency will also shift to front and behind when the radius changes. But levels of outputs (port 2 and port 3) are not affected by this radius value.

Analysis 2

- Parameter : R_2
- Optimum value : $R_2 = 12$ mm
- Step-down value : $R_2 = 11$ mm
- Step-up value : $R_2 = 13$ mm

Result:

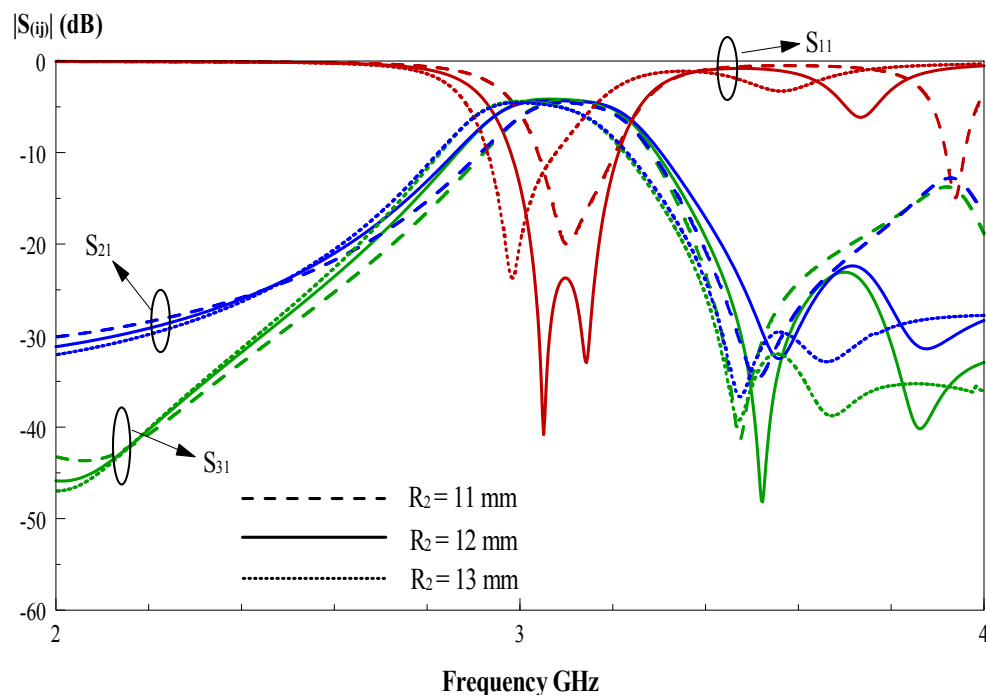


Figure 4.8: Effect of radius R_2 on the proposed resonator

When the radius of second patch changes, the two-modes of S_{11} was combine together. But when the radius value step-up to 13 mm, the frequency is shift to 3 GHz which is we needed but it there is only one pole exists. The radius was chosen to be optimum value 12 mm to maintain the two-mode input matching.

Analysis 3

- Parameter : R_3
- Optimum value : $R_3 = 8$ mm
- Step-down value : $R_3 = 7$ mm
- Step-up value : $R_3 = 9$ mm

Result:

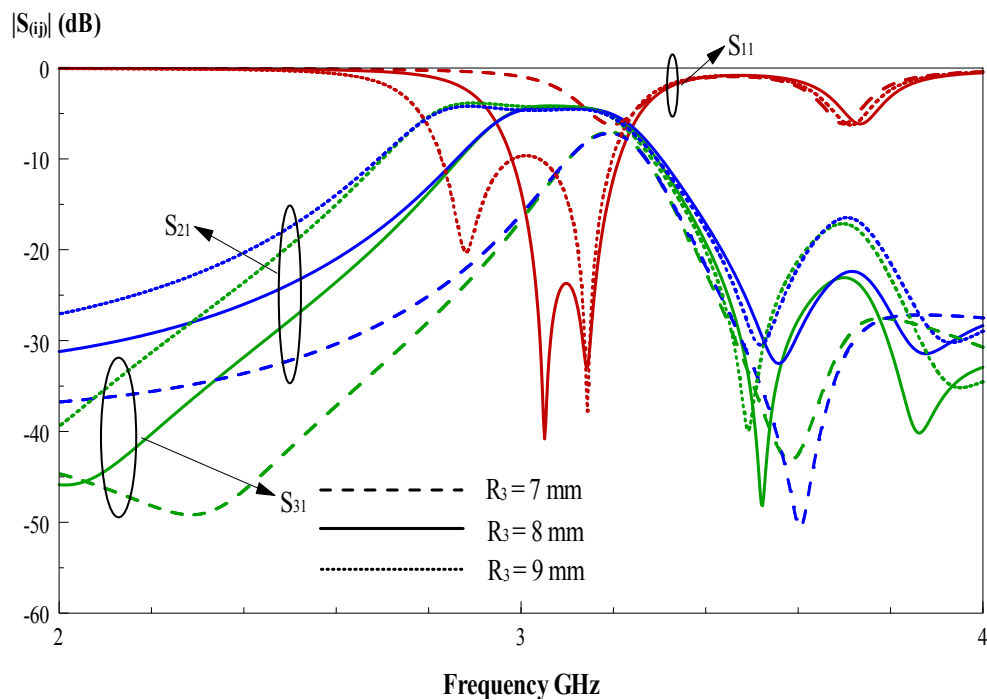


Figure 4.9: Effect of radius R_3 on the proposed resonator

From the figure 4.9, it shows that the results for input impedance was look very nice when the radius of the middle slot was step-up to 9 mm. It has wider bandwidth and the center frequency at 3 GHz, but the input impedance level was higher than 12 dB. On the other hand, the radius value step-down to 7 mm, the S_{11} was become badly. So the optimum value of radius for the slot to be 8 mm.

Analysis 4

- Parameter : W_1
- Optimum value : $W_1 = 1.75$ mm
- Step-down value : $W_1 = 1.65$ mm
- Step-up value : $W_1 = 1.85$ mm

Result:

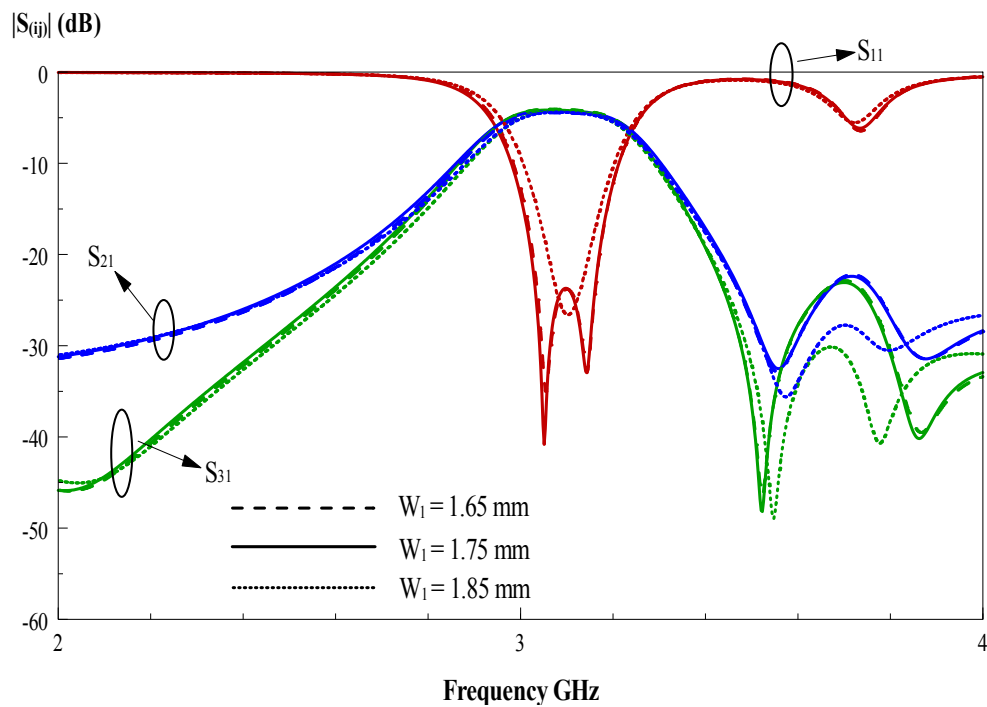


Figure 4.10: Effect of width W_1 on the proposed resonator

In figure, when the width W_1 is decreased to 1.65 mm, there is not affect for the S_{11} . But when increase W_1 to 1.85 mm, the mode of S_{11} was combined together. The magnitude of output port is not affected much when W_1 changes.

Analysis 5

- Parameter : W_2
- Optimum value : $W_2 = 1.7$ mm
- Step-down value : $W_2 = 1.6$ mm
- Step-up value : $W_2 = 1.8$ mm

Result:

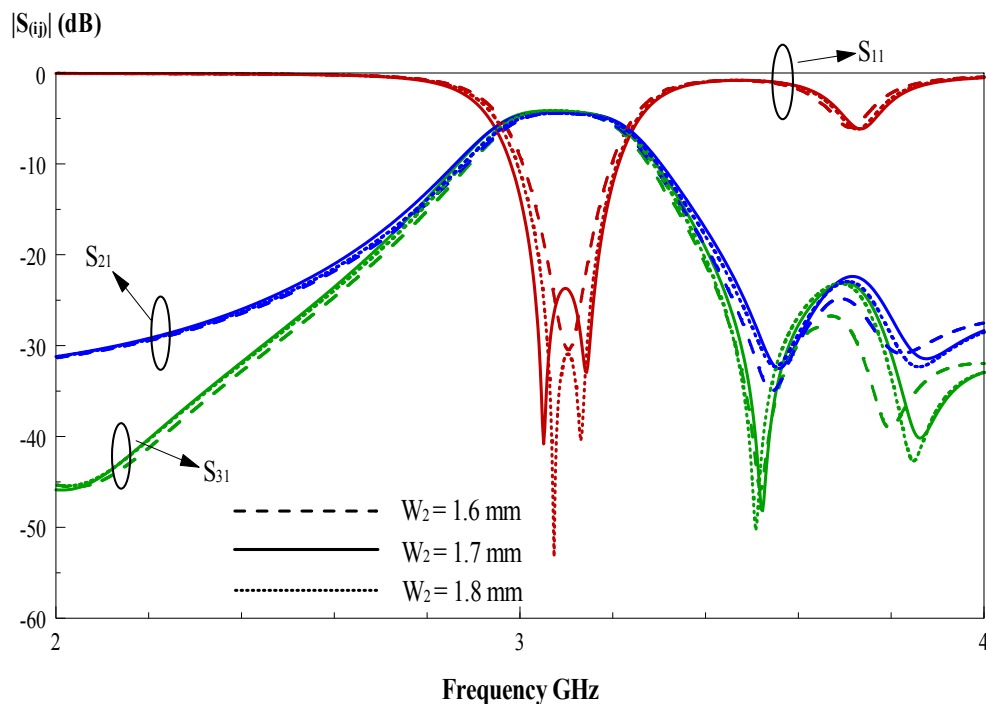


Figure 4.11: Effect of width W_2 on the proposed resonator

Parameter W_2 does not bring much effect on the proposed resonator. It introduces shift in the position of poles of the resonator when the width is altered. As can be seen in Figure 4.11, the optimum value of W_2 gives the best reflection coefficient S_{11} . Apart from that, it has no significant effect on output port.

Analysis 6

- Parameter : W_3
- Optimum value : $W_3 = 1.7$ mm
- Step-down value : $W_3 = 1.6$ mm
- Step-up value : $W_3 = 1.8$ mm

Result:

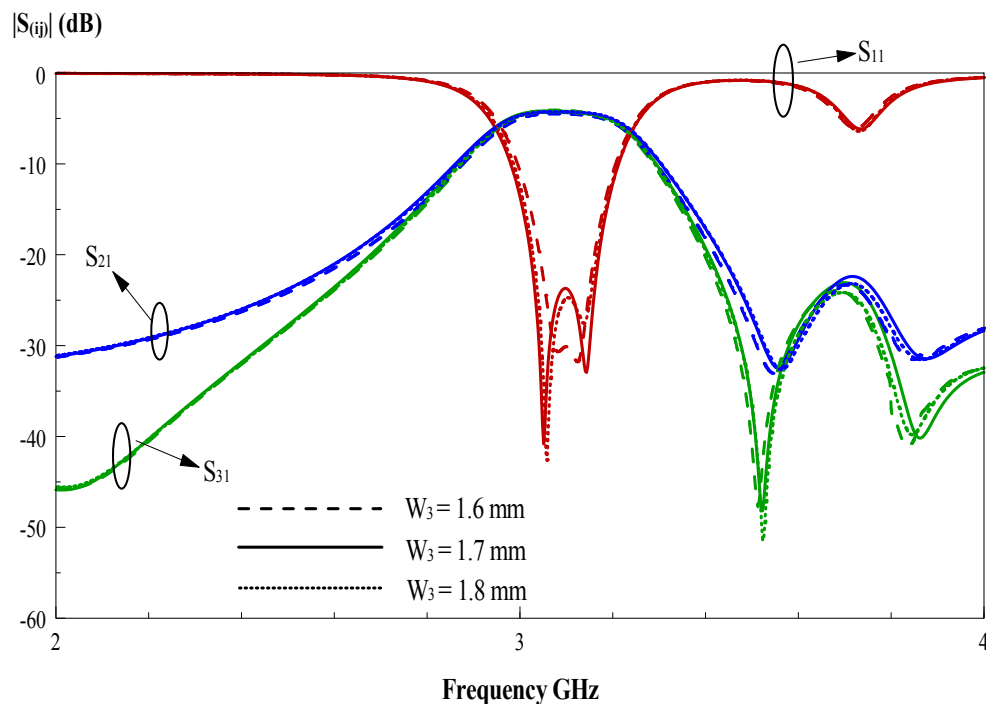


Figure 4.12: Effect of width W_3 on the proposed resonator

The result of W_3 is same as the results of W_2 . There are not many changes when the width was changes. Just the mode of input port was combined together when the width step-down to 1.6 mm.

Analysis 7

- Parameter : S_1
- Optimum value : $S_1 = 70$ mm
- Step-down value : $S_1 = 50$ mm
- Step-up value : $S_1 = 80$ mm

Result:

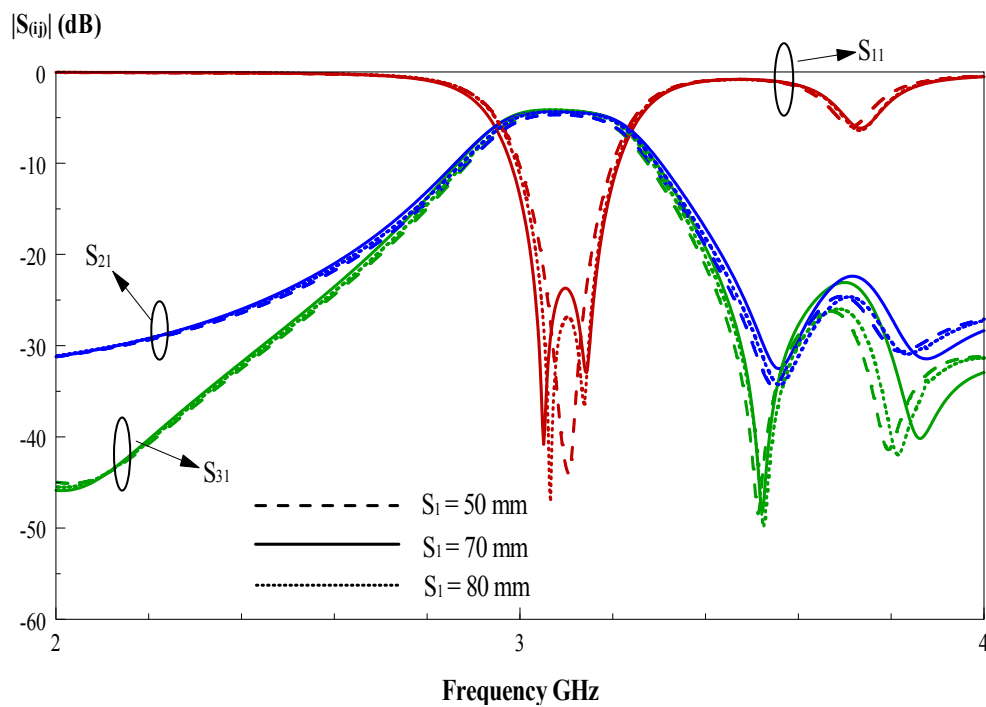


Figure 4.13: Effect of size S_1 on the proposed resonator

The S_1 does not affect the result much just the position of the poles was shift to left when the size step-up to 80 mm. When size was step-down to 50 mm, two-poles was combined together. This is not an important parameter if only changes this parameter.

Analysis 8

- Parameter : S_2
- Optimum value : $S_2 = 70$ mm
- Step-down value : $S_2 = 50$ mm
- Step-up value : $S_2 = 80$ mm

Result:

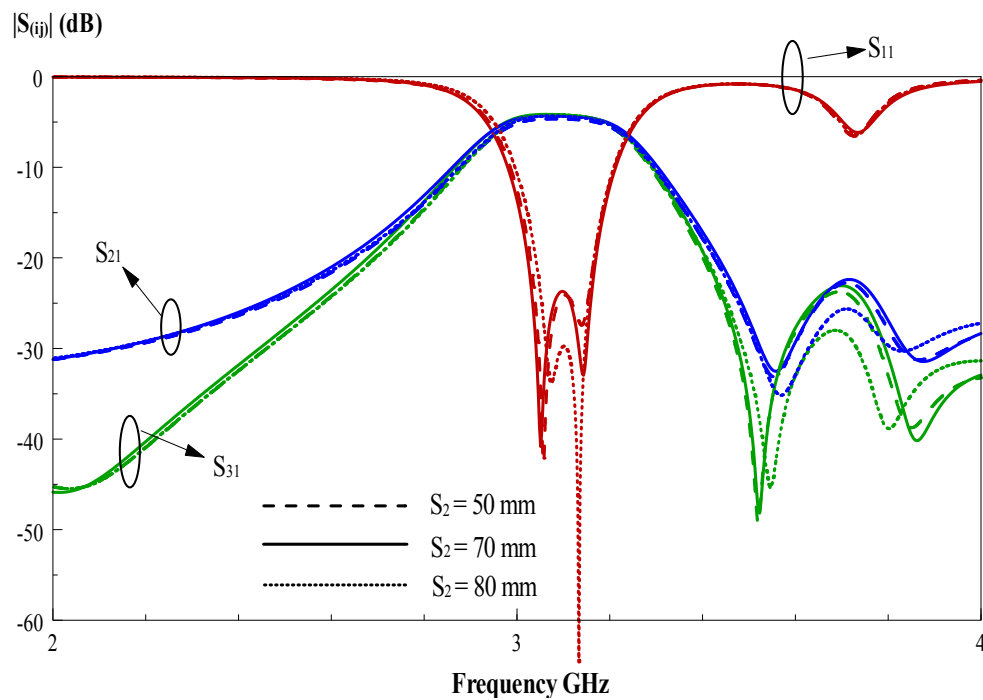


Figure 4.14: Effect of size S_2 on the proposed resonator

Result for this parameter is same as S_1 . There are not much affect when S_2 value increase or decrease. Positions of two poles are shift to right.

Analysis 9

- Parameter : S_1, S_2
- Optimum value : $S_1 = S_2 = 70$ mm
- Step-down value : $S_1 = S_2 = 50$ mm
- Step-up value : $S_1 = S_2 = 80$ mm

Result:

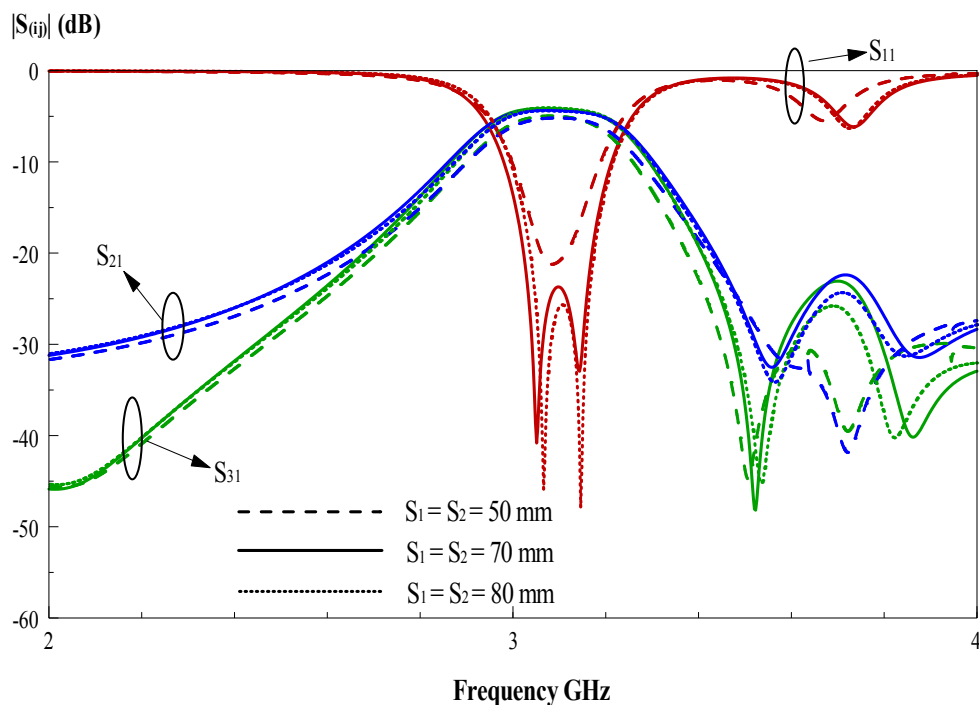


Figure 4.15: Effect of size S_1 and S_2 on the proposed resonator

But when the size S_1 and S_2 of the substrate change together to 50 mm, the two poles was combined become single poles which at the center frequency. While, there are not much changes when the size step-up to 80 mm.

Analysis 10

- Parameter : R_1, R_2
- Optimum value : $R_1 = 13 \text{ mm}, R_2 = 12 \text{ mm}$
- Step-down value : $R_1 = R_2 = 12 \text{ mm}$
- Step-up value : $R_1 = R_2 = 14 \text{ mm}$

Result:

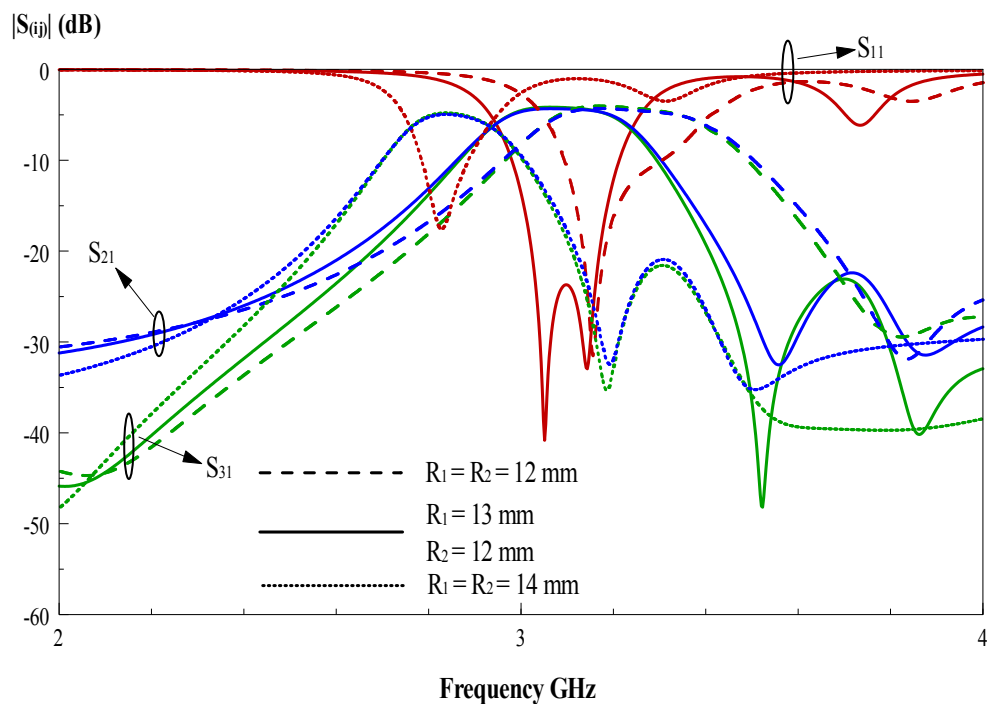


Figure 4.16: Effect of radius R_1 and R_2 on the proposed resonator

When the radius of the top layers same as the bottom layer, the results was become badly. It may due to the signal from input port be able to pass the signal with effectively to bottom layer. So we can conclude that the radius of top patch and bottom patch cannot be the same size.

Analysis 11

- Parameter : W_1, W_2, W_3
- Optimum value : $W_1 = 1.75 \text{ mm}, W_2 = W_3 = 1.70 \text{ mm}$
- Step-down value : $W_1 = W_2 = W_3 = 1.70 \text{ mm}$
- Step-up value : $W_1 = W_2 = W_3 = 1.75 \text{ mm}$

Result:

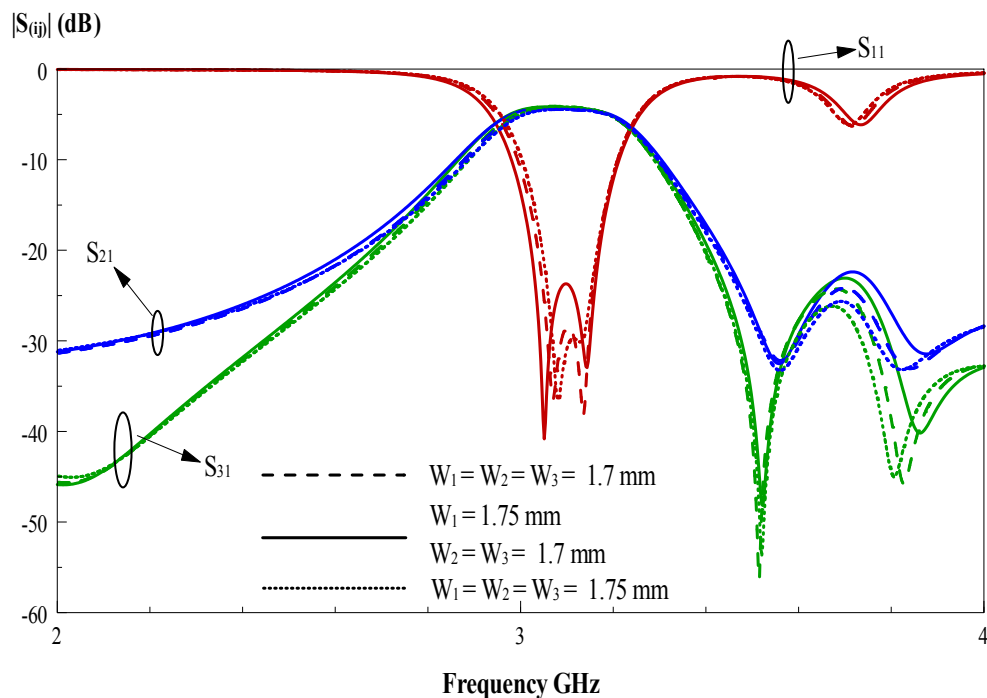


Figure 4.17: Effect of width W_1, W_2 and W_3 on the proposed resonator

In the figure above, the width of input port and output port was not affect much when three of them in the same width. But the characteristics impedance, Z_o of the output port may not equal to 50Ω .

Analysis 12

- Parameter : H_1
- Optimum value : $H_1 = 0.8128$ mm
- Step-up value : $H_1 = 1.5240$ mm

Result:

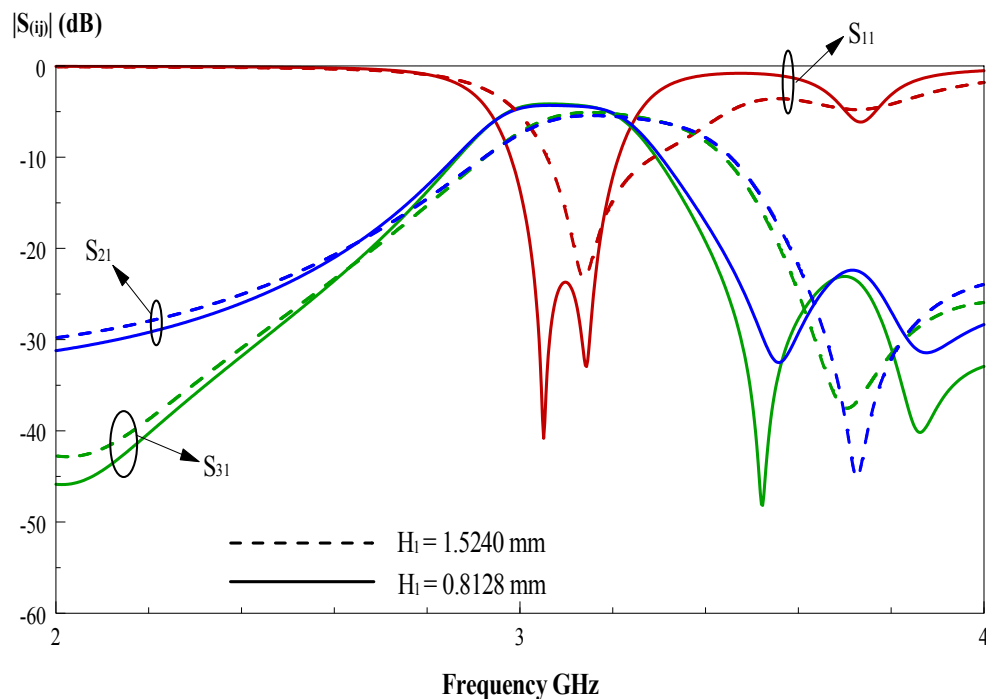


Figure 4.18: Effect of thickness H_1 on the proposed resonator

Apart from that, from figure 4.18, the substrate thickness with 0.8128 mm was the best. It may be due to the gap between the top patch and bottom patch cannot be too large to avoid the signal could not pass through.

Analysis 13

- Parameter : G_1
- Optimum value : $G_1 = 0.5$ mm
- Step-down value : $G_1 = 0.2$ mm
- Step-up value : $G_1 = 1.0$ mm

Result:

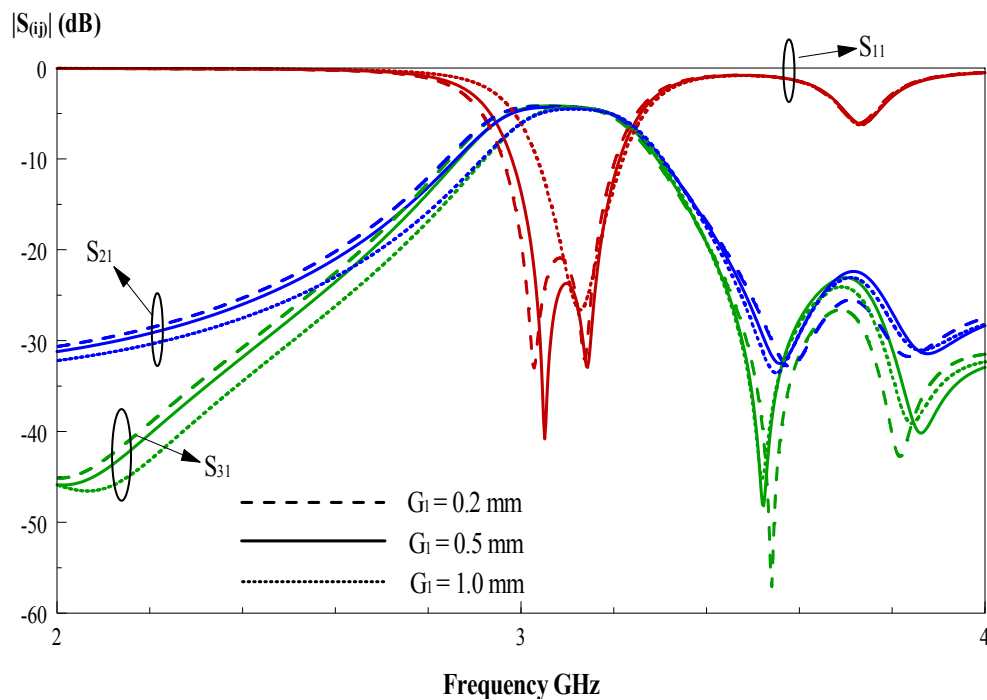


Figure 4.19: Effect of gap G_1 on the proposed resonator

As can be seen in the figures, we can clearly see that the gap G_1 plays an important role in deciding how much signal passes through the resonator is. More signal power is received at the output ports when the vertical gaps between two sectorial slots are closer. Here, the gap g_1 is chosen to be 0.50 mm so that the reflection coefficient S_{11} is less than 12 dB.

Analysis 14

- Parameter : G_2
- Optimum value : $G_2 = 0.5$ mm
- Step-down value : $G_2 = 0.2$ mm
- Step-up value : $G_2 = 1.0$ mm

Result:

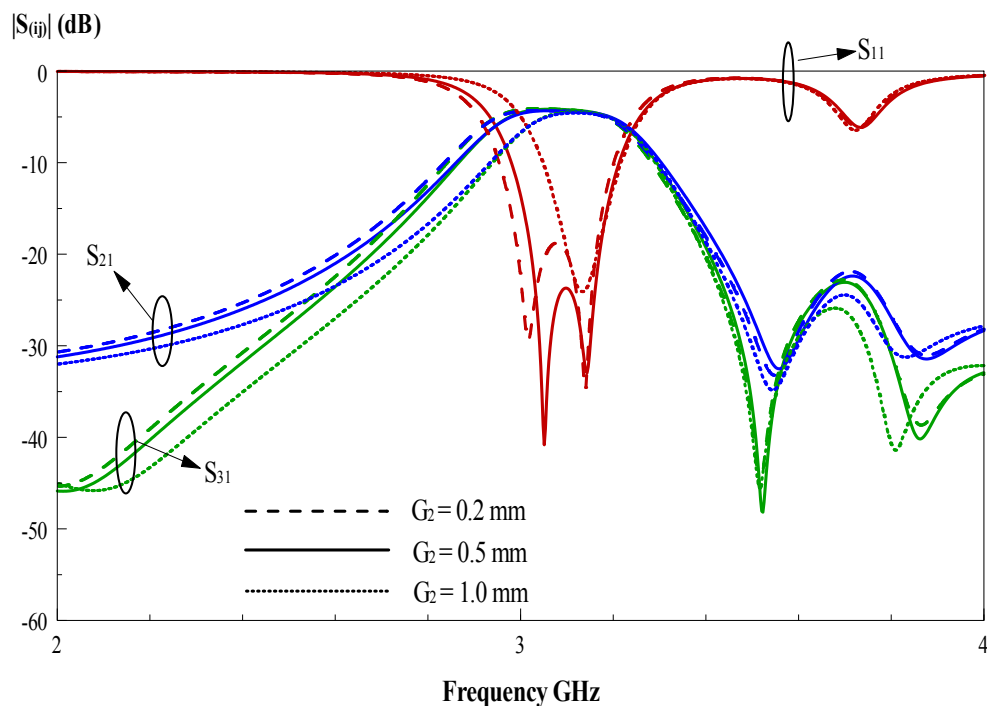


Figure 4.20: Effect of gap G_2 on the proposed resonator

Parameter G_2 has the same effect as that for G_1 . More signal power is received at the output ports when the horizontal gaps between two sectorial slots are closer. Here, the gap G_2 is chosen to be 0.50 mm so that the reflection coefficient S_{11} is less than 12 dB.

Analysis 15

- Parameter : G_1, G_2
- Optimum value : $G_1 = G_2 = 0.5$ mm
- Step-down value : $G_1 = G_2 = 0.2$ mm
- Step-up value : $G_1 = G_2 = 1.0$ mm

Result:

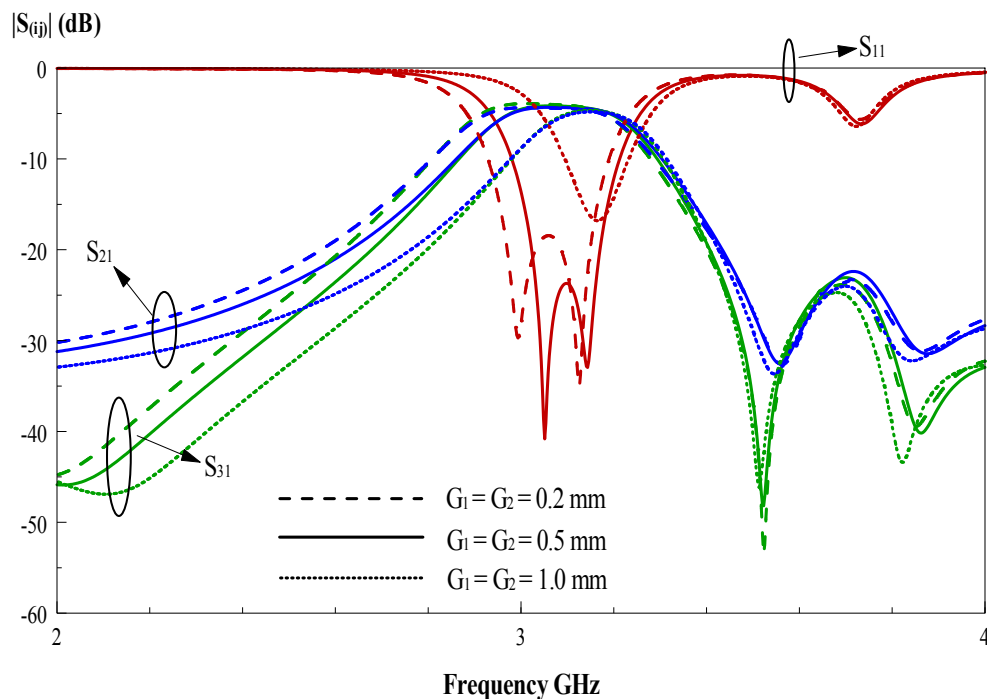


Figure 4.21: Effect of gap G_1 and G_2 on the proposed resonator

By controlling the vertical and horizontal gaps between two sectorial, the smaller the gap the frequency was shift nearer to 3 GHz. But the gap cannot be too small because during the fabrication, the gaps are very easily over etched.

CHAPTER 5

CONCLUSION AND RECOMMENDATIONS

5.1 Achievement

In this project, a broadside-coupled patch directional coupler has been proposed and investigated in Chapter 3. By using proposed directional coupler shown in figure 3.1, a two-mode directional coupler can be designed. Idea was demonstrated on the RO4003C substrate. Experimental data are compared with the simulation results. Fractional bandwidth difference between experimental and simulation is 9.2% which is less than 10%. This two-mode directional coupler has wideband performance and two poles in S_{11} .

A travelling-wave sectorial slot resonator has been proposed and discussion in Chapter 4. Proposed design was further demonstrated on RO4003C substrate. The simulation data were discussed by comparing parameter analysis due to experiments is run out of time. A 12 dB return loss was achieved so that signal pass through the device are not easy reflected back.

5.2 Future Work

As for the proposed multi-port directional, the coupling level very difficult to maintain in 10 ± 1 dB during the experiment stages. It may due the alignment of the layer which is not same as simulation alignment. Therefore, as for future

improvement, the coupled line can be separated to two U-shaped to make the circuit compact. So the circuit total has six-port directional coupler to achieved better coupling level.

For the proposed resonator, design can be improve by using smaller size of substrate such as 50 x 50 mm which can save the cost of board. Apart from that, to achieve the center frequency at 3 GHz, top and bottom patch should enlarge. This proposed resonator can be a strong travelling wave if center frequency meets the Federal Communications Commission (FCC) requirement.

5.3 Conclusion

Both broadside-coupled patch directional coupler and travelling-wave slot resonator have been designed and demonstrated in this project. For the proposed directional coupler, experimental results agree well with the simulation results. While, for proposed resonator, only simulation can be done. Experiments cannot be finis due to author is run out of time. In this thesis, design considerations and issues of the proposed directional coupler and resonator have also been studied. The objectives of this project have been met.

REFERENCES

Directional Couplers. (n.d.). Retrieved August 17, 2012, from Microwave Encyclopedia: www.microwaves101.com/encyclopedia/directionalcouplers.cfm.

Pozar, D. M. (1998). *Microwave Engineering*. Canada: John Wiley & Sons, Inc.

S.N.A.M. Ghazali, N.Seman, R.C. Yob, M.K.A. Rahim and S.K.A.Rahim. (November 2011). Design and Cross-Section Analysis of Wideband Rectangular-Shaped Directional Coupler. *IEEE transaction on Microwave Theory and Techniques*.

H.-J. Yuan and Y. Fan. (November 2011). Compact Microstrip Dual-band Filter with Stepped-impedance Resonators. *Electronic Letters*.

Ferdinando Alessandri, Marco Giordano, Marco Guglielmi, Giacomo Martirano, Francesco Vitulli. (May 2003). A New Multiple-Tuned Six-Port Riblet-Type Directional Coupler in Rectangular Waveguide. *IEEE Transactions on Microwave Theory and Techniques*, Vol. 51, No.5.

Chang, K. *RF and Microwave Wireless System*. New York/ Chichester/ Weinheim/ Brisbane/ Singapore/ Toronto: John Wiley & Sons, Inc.

Introduction to RF & Wireless Communications Systems. (n.d.). Retrieved August 18, 2012, from National Instruments: <http://www.ni.com/white-paper/3541/en>.

Microstrip. (n.d.). Retrieved August 18, 2012, from Wikipedia: <http://en.wikipedia.org/wiki/Microstrip>.

Hong J. S. & M.J. Lancaster. . (2001). *Microstrip Filter for RF/Microwave Applications*. New York/ Chichester/ Weinheim/ Brisbane/ Singapore/ Toronto: John Wiley & Sons, Inc.

J.K. Shimizu, E. M. T. Jones. (1958). Coupled-Transmission-Line Directional Coupler. *IEEE Transactions on Microwave Theory and Techniques* , 404.

Resonator. (n.d.). Retrieved August 20, 2012, from Wikipedia: <http://en.wikipedia.org/wiki/Resonator>.

Chapter 6 Microwave Resonators. (n.d). Retrieved August 21, 2012, from: http://cc.ee.ntu.edu.tw/~thc/course_mckt/note/note5.pdf.

An Introduction to Microwave Technology. (n.d). Retrieved August 21, 2012, from: <http://www.invictusnetworks.com/faq/RF%20Technical%20Info%20and%20FCC%20Regs/An%20Introduction%20to%20Microwave%20Technology.pdf>.

Characteristic impedance (n.d), obtained at 25 August 2012, http://en.wikipedia.org/wiki/Characteristic_impedance

Microstrip Substrate Relative Dielectric Constant (December 2007), obtained at 26 August 2012. <http://www.mwrf.com/Articles/Index.cfm?Ad=1&ArticleID=17725>

Juan Enrique Page, Jaime Esteban and Carlos Camacho-Penalosa. (n.d.). Lattice Equivalent Circuits of Transmission-Line and Coupled-Line Section. *IEEE Transaction on Microwave Theory and Techniques*

Bian Wu, Wen Su, Shou-jia Sun and Chang-Hong Liang. (November 2011). Novel Dual-mode Bandpass Filter Using Slot-line Square Loop Resonator. *IEEE transaction on Microwave Theory and Techniques*.

C. –C. Chang, C. Caloz and T. Itoh. (2011). Analysis of a Compact Slot Resonator in the Ground Plane for Microstrip Structures. *IEEE transaction on Microwave Theory and Techniques*.

J-L. Li, S.-W Qu and Q. Xue. (February 2007). Microstrip directional coupler with flat coupling and high isolation. *Electronic Letters* , Vol. 43, No. 4.

Ravi Kumar, Rajesh Kumar Vishwakarma and Ashutosh Singh. (2008). Analysis of Aperture Coupled Multilayered Microstrip Directional Coupler. *IEEE transaction on Microwave Theory and Techniques*.

Ruscito and Elizabeth. (September 2011). Application of a High Q, Low Cost Hemispherical Cavity Resonator to Microwave Oscillators. *ProQuest Dissertation and Thesis*.

Kun Song, Yingzeng Yin, Shoutao Fan and Yuqing Wei. (2011). Compact UWB Band-pass Filter with Ring Slot Resonator Structure for Improved Upper Stop-band Suppression Characteristic. *IEEE transaction on Microwave Theory and Techniques*.